Permeation Through an Open Channel: Poisson-Nernst-Planck Theory of a Synthetic Ionic Channel

Duan Chen,* James Lear, and Bob Eisenberg*

*Department of Molecular Biophysics and Physiology, Rush Medical College, Chicago, IL 60612, and Department of Biochemistry and Biophysics, University of Pennsylvania, Philadelphia, PA 19104-6059 USA

ABSTRACT   The synthetic channel [acetyl-(LeuSerSerLeuLeuSerLeu)$_3$-CONH$_2$]$_6$ (pore diameter ~8 Å, length ~30 Å) is a bundle of six α-helices with blocked termini. This simple channel has complex properties, which are difficult to explain, even qualitatively, by traditional theories: its single-channel currents rectify in symmetrical solutions and its selectivity (defined by reversal potential) is a sensitive function of bathing solution. These complex properties can be fit quantitatively if the channel has fixed charge at its ends, forming a kind of macrodipole, bracketing a central charged region, and the shielding of the fixed charges is described by the Poisson-Nernst-Planck (PNP) equations. PNP fits current voltage relations measured in 15 solutions with an r.m.s. error of 3.6% using four adjustable parameters: the diffusion coefficients in the channel's pore D_K = 2.1 × 10^{-6} and D_{Cl} = 2.6 × 10^{-7} cm^2/s; and the fixed charge at the ends of the channel of ±0.12e (with unequal densities 0.71 M = 0.021e/Å on the N-side and −1.9 M = −0.058e/Å on the C-side). The fixed charge in the central region is 0.31e (with density P_2 = 0.47 M = 0.014e/Å). In contrast to traditional theories, PNP computes the electric field in the open channel from all of the charges in the system, by a rapid and accurate numerical procedure. In essence, PNP is a theory of the shielding of fixed (i.e., permanent) charge of the channel by mobile charge and by the ionic atmosphere in and near the channel's pore. The theory fits a wide range of data because the ionic contents and potential profile in the channel change significantly with experimental conditions, as they must, if the channel simultaneously satisfies the Poisson and Nernst-Planck equations and boundary conditions. Qualitatively speaking, the theory shows that small changes in the ionic atmosphere of the channel (i.e., shielding) make big changes in the potential profile and even bigger changes in flux, because potential is a sensitive function of charge and shielding, and flux is an exponential function of potential.

INTRODUCTION

Ionic channels are gatekeepers to cells, controlling biological processes of considerable generality and importance (Hille, 1992), but the physics underlying their function is simple, as is their structure. Once open, ionic channels form a nearly one-dimensional path for electrodiffusion. We adopt the simplest self-consistent[1] theory of electrodiffusion and call it PNP for short: Poisson's equation to describe how the charge on ions and proteins determines the potential of the electric field and Nernst-Planck equations to describe the migration and diffusion of ions in gradients of potential and concentration. Combined, these are the "drift-diffusion equations" of physics (see Mason and McDaniel, 1988; Spohn, 1991; Balian, 1992) particularly solid state physics (Jerome, 1996; Ashcroft and Mermin, 1976; Seeger, 1991; Shur, 1990; Sze, 1981; Selberherr, 1984; Roulston, 1990; Lundstrom, 1992). Eisenberg (1996a) gives other references and reviews the biological literature. The drift-diffusion equations compute the electric field (and thus shielding), unlike most other theories of the open channel, which assume it.[2]

The PNP equations are a mean field theory that occupies. the same place in the hierarchy of approximations of condensed phases as the Vlasov equations[3] of plasma physics (Balescu, 1975, p. 404; Balian, 1992; Kersch and Morokoff, 1995; see also, Balescu, 1963) and the nonlinear Poisson Boltzmann theory of solutions and proteins (Honig and Nicholls, 1995; Davis and McCammon, 1990; Hecht et al., 1995) is particularly important because it provides direct experimental verification of the theory (see also Warwicker and Watson, 1982; Klapper et al., 1986; Gilson et al., 1988; Davis et al., 1991; Holst et al., 1994; Forsten et al., 1994, describe important computational improvements to the theory). Poisson-Boltzmann is, however, an equilibrium theory that does not allow flux, or nonequilibrium states of the system. It could thus describe only perfectly selective channels held at their equilibrium potential. An equilibrium theory is of limited use in describing the purposeful function of transistors (e.g., as logic elements) and has similar limitations in describing channels. Both transistors and channels after all must be biased to perform their useful work: without the flux that accompanies bias, transistors cannot amplify or switch; without the flux that accompanies bias, channels cannot transport current or ions and so cannot change the membrane potential or cell contents.

In the PNP theory of channels, permanent (i.e., often called fixed) charge plays a particularly important role, as it does in transistors, where (under the name doping) it determines the nature and properties of the semiconductor device. In both cases, the permanent charge profile $P(x)$ is a

one-dimensional representation of the effective charge of the underlying (protein or crystal) structure that does not change in a wide range of conditions. Indeed, once the distribution of permanent charge is known, the PNP equations predict the properties of the open channel—the fluxes and current through it—in all experimental conditions of varying concentrations and transmembrane potentials.[4]

In the simple version of the PNP equations used here, structural parameters change only if the channel protein changes its conformation or composition: the radius and length of the channel, the dielectric constants, the diffusion coefficients, and the distribution of permanent charge all remain fixed as solutions and transmembrane potential are varied. Conformations of proteins undoubtedly can and do change as conditions change. Their composition can change as well: proteins can donate (or accept) a hydrogen (a process sometimes called ionization) or a phosphate group (called phosphorylation), thus changing their permanent charge, and probably shape and conformation as well, and perhaps thereby gating the channel. Nonetheless, in this paper, the structure and distribution of the permanent charge of the channel are kept fixed as solutions and transmembrane potential vary. We wish to see how well a fixed version of the theory, describing a channel of one conformation and composition, can predict such changeable data.

Here we consider the channel made by the synthetic protein that is a bundle of six amphiphilic α-helices [acetyl-(LeuSerSerLeuLeuSerLeu)$_3$-CONH$_2$]$_6$ with an acetylated amino as the N-terminal group and a carboxamide as the C-terminal group, both formally uncharged (Åkerfeldt et al., 1993). LS (as we call it) was designed (Lear et al., 1988) to be a bundle of α-helices that can be described more or less as a macrodipole (Wada, 1976; Hol, 1985). Strictly speaking, a macrodipole is a spatial distribution of fixed (i.e., permanent) charge rather like a dumbbell, made of equal and oppositely signed charges near the ends of a cylindrical molecule, bracketing a central charge-free region. Speaking less strictly, the central region might contain a uniform density of charge, arising, for example, from the hydroxyls of serine residues.[5] Still less strictly, the end charges might be inherently unequal (Åqvist et al., 1991; Sitkoff et al., 1994, and references cited therein), or they might be effectively unequal if, for example, charged headgroups of adjacent lipid molecules produced significant shielding.

Placed in a lipid bilayer, LS makes a channel 30 Å long with a pore diameter of 8 Å (Kienker et al., 1994; Kienker and Lear, 1995), reminiscent of natural channels. The selectivity of LS (as traditionally defined by the reversal potential) varies substantially with bathing solution. Interestingly, the single channel shows strong N-ward rectification (i.e., more current flows from C-terminal to N-terminal than vice versa: Kienker et al., 1994; Kienker and Lear, 1995), even in symmetrical solutions, where the gradient of electrochemical potential is nearly zero.

We loosely describe the permanent charge at the ends of the channel as a macrodipole (using one adjustable parameter), bracketing permanent charge in the central region

(described by one other parameter), and show that the PNP equations can predict the wide range of behavior observed experimentally as solutions and membrane potentials are varied, if two additional parameters are used to describe the diffusion of K$^+$ and Cl$^-$ in the channel's pore. The *IV* curves predicted from this distribution of permanent charge rectify in symmetrical solutions. In particular, the reversal potential (the potential at which zero current flows through the channel) changes dramatically as solutions are changed, even if, for example, solutions are simply interchanged from one side of the channel to another: the selectivity of the predicted channel changes as solutions are changed.

THEORY AND METHODS

We present PNP theory here to make the paper reasonably self-contained, following the suggestion of the reviewers and the editor, although nearly the same presentation has been published in the review of Eisenberg (1996a) that summarized the original papers (e.g., Chen and Eisenberg, 1993a,b).

The program that executes this numerical procedure is written in FORTRAN 77 and is available to anyone who requests it. The program has been compiled and run easily on a number of systems, and we think it (or its equivalent) is needed to develop a qualitative feel for the PNP equations: the system is so nonlinear (see Fig. 11) that we find it necessary (for physical understanding and subsequent biological intuition) to actually compute and plot the potential profiles and concentration profiles, for every membrane potential and pair of concentrations of interest.

The channel is described in this theory as a one-dimensional structure of radius r and length d, extending from $x = 0$ on the L (or left or N or inside of the channel) to $x = d$ on the R (or right or C or outside). The baths extend to infinity where the concentrations of ions $C_j(-\infty) \equiv C_j(L)$ and $C_j(+\infty) \equiv C_j(R)$ (units: cm^{-3}) and the potentials (units: volts) $\varphi(-\infty) \equiv \varphi(L)$ are maintained at desired values by the experimenter and his apparatus.[6] Theoretical expressions are written in terms of dimensionless potential functions $\Phi(\cdot)$, and the (dimensional) potential difference V_{appl} applied to the baths, which we often loosely call the transmembrane potential, following laboratory practice (see Eq. 4):

$$\Phi(\cdot) \equiv \frac{e\varphi(\cdot)}{k_B T} = \frac{F\varphi(\cdot)}{RT} \tag{1}$$

$$V_{appl} \equiv \varphi(L) - \varphi(R).$$

Usually $\varphi(+\infty) \equiv \varphi(R) = 0$ and $\varphi(L) = V_{appl}$. Here, e is the charge on a proton; F is Faraday's constant, the charge on Avogadro's number of protons; the thermal energy $k_B T$ or RT is given by the product of T, the absolute temperature in degrees Kelvin, and k_B, the Boltzmann constant, or R, the gas constant.

Donnan potential

Permanent (i.e., fixed) charge at the ends of the channels $P(0)$ and $P(d)$ creates Donnan or built-in potentials in the baths $\Phi_{bi}(0)$, $\Phi_{bi}(d)$, assumed independent of current flow. With this approximation,[7] these are easily computed because the bathing solutions are made of (nearly) equal amounts of cations and anions, viz., $\Sigma_j z_j C_j(L) = \Sigma_j z_j C_j(R) = 0$. Then,

$$\Phi_{bi}(0) \equiv \log_e \frac{\sqrt{P^2(0) + 4C_1(L)C_2(L)} + P(0)}{2C_2(L)} \tag{2}$$

$$\Phi_{bi}(d) \equiv \log_e \frac{\sqrt{P^2(d) + 4C_1(R)C_2(R)} + P(d)}{2C_2(R)}. \tag{3}$$

The potentials on each end of the pore, and from one end to the other, are

$$\Phi(0) = \Phi_{bi}(0) + \frac{e}{k_B T} V_{appl}$$

$$\Phi(d) = \Phi_{bi}(d) \tag{4}$$

$$\Delta \equiv V_{appl} + \varphi_{bi}(0) - \varphi_{bi}(d).$$

Note that the potential Δ (between $x = 0$ and $x = d$) is not the transmembrane potential V_{appl} measured between the electrodes (i.e., between $x = L \to -\infty$ and $x = R \to +\infty$) that is used as the independent variable in most measurements of IV relations.

The concentrations just outside the channel $C_j(0)$ and $C_j(d)$ can easily be computed because the baths are assumed at equilibrium, even when current flows, so

$$C_j(0) = C_j(L)\exp[-z_j\Phi_{bi}(0)]$$

$$C_j(d) = C_j(R)\exp[-z_j\Phi_{bi}(d)]. \tag{5}$$

Thus the permanent charge at the ends of the channel $P(0)$ and $P(d)$ are used to compute the potential drop between the electrodes (at $\pm\infty$) and the ends of the channel (using Eqs. 2 and 3). The potential drops are then used to compute the concentrations at the ends of the channel.

Poisson's equation[8] determines the potential from the charges present:

$$-\varepsilon_w\varepsilon_0\frac{d^2\varphi}{dx^2} = \overbrace{eP(x)}^{\substack{\text{Permanent} \\ \text{charge}}} + \overbrace{e\sum_j z_j C_j(x)}^{\substack{\text{Channel} \\ \text{contents}}} + \overbrace{\bar{\varepsilon}[\Delta(1 - x/d) - \varphi(x)]}^{\substack{\text{Induced charge}}}.$$

$$\underbrace{\qquad\qquad\qquad\qquad\qquad\qquad}_{\substack{\text{Deviation from} \\ \text{constant field}}} \tag{6}$$

The concentrations $P(x)$ and $C_j(x)$ are one-dimensional representations of numbers of particles per unit volume (e.g., cm^{-3}). They are effective concentrations. The dielectric properties of the channel protein and its watery pore (radius r, length d) are described by the permittivity of free space ε_0 (units: coulombs $\cdot$ volt^{-1} $\cdot$ cm^{-1}); the (dimensionless) dielectric constants ε_p and ε_{H_2O}, respectively; and the effective dielectric parameter[9] $\bar{\varepsilon}$ (units: coulombs $\cdot$ volt^{-1} $\cdot$ cm^{-3}):

$$\bar{\varepsilon} \equiv \frac{\varepsilon_p}{\varepsilon_{H_2O}} \cdot \frac{2\varepsilon_0}{r^2\ln(d/r)}. \tag{7}$$

Nernst-Planck equations determine the flux J_j (units: cm^{-2} $\cdot$ s^{-1}) of each ion j,

$$J_j = -D_j\left[\overbrace{\frac{dC_j}{dx}}^{\text{Diffusion}} + \overbrace{z_jC_j(x)\frac{d\Phi}{dx}}^{\text{Migration}}\right], \tag{8}$$

where D_j is its diffusion coefficient.

The Nernst-Planck equations (Eq. 8) can be integrated analytically to give expressions for the concentration of ions in the channel, namely the channel's contents:

$$C_j(x) = \frac{C_j(0) \cdot \exp z_j[\Phi(0) - \Phi(x)] \cdot \int_x^d \exp z_j\Phi(\zeta)d\zeta}{\int_0^d \exp z_j\Phi(\zeta)d\zeta}$$

$$+ \frac{C_j(d) \cdot \exp z_j[\Phi(d) - \Phi(x)] \cdot \int_0^x \exp z_j\Phi(\zeta)d\zeta}{\int_0^d \exp z_j\Phi(\zeta)d\zeta}. \tag{9}$$

This system of equations (Eqs. 6 and 9) must be solved simultaneously because the potential depends on the concentrations $C_j(x)$ through the Poisson equation (Eq. 6), but the concentrations also depend on the potential through the integrated Nernst-Planck equations (Eq. 9). Indeed, the concentrations depend exponentially on the potential.

A different integration of the Nernst-Planck equations shows that flux and current I also depend exponentially on the potential profile:

$$J_j = D_j\frac{C_j(L)\exp(z_jV_{appl}/k_BT) - C_j(R)}{\int_0^d \exp z_j\Phi(x)dx}; \qquad I = \pi r^2 \cdot \sum_j ez_j J_j, \tag{10}$$

which can be rewritten to emphasize the symmetry of the problem:

$$J_j = D_j\frac{C_j(L)}{\int_0^d \exp z_j[\Phi(x) - z_jV_{appl}/k_BT]dx}$$

$$- D_j\frac{C_j(R)}{\int_0^d \exp z_j\Phi(x)dx}. \tag{11}$$

The Nernst-Planck equations can be derived from the stochastic description of the motion of a single charged particle. Eisenberg et al. (1995) prove that

$$\frac{\exp(z_jV_{appl}/k_BT)}{1/d\int_0^d \exp z_j\Phi(x)dx} \equiv \text{Prob}\{R|L\};$$

$$\frac{1}{1/d\int_0^d \exp z_j\Phi(x)dx} \equiv \text{Prob}\{L|R\}. \tag{12}$$

They show that the concentrations $C_j(x)$ describe the mean values of the probability of an ion being at location x: the Nernst-Planck equation is not a (perhaps vaguely derived) continuum approximation, but rather an exact description of the probability density function of the location of discrete particles.

Equation 11 predicts the charge accumulated in the patch pipette or electrode during the sampling time of the current measurement, typically 5–50 μs. Because the passage time of trajectories is much faster than that (160 ns for a channel that always contains one ion and passes 1 pA of current; see similar estimates from the simulations of Cooper et al., 1985; Chiu and Jakobsson, 1989; Barcilon et al., 1993; Eisenberg et al., 1995) and atomic motions are very much faster yet (ranging from 10^{-14} s for solvation (Stratt, 1995) to, say, 10^{-11} s for motions of the atoms of the protein), the current measurement is necessarily an average of a large number of individual stochastic events. The potential that describes this averaged current must then also be an averaged potential (some sort of "potential of mean force"), and the parameters linking potential and current (e.g., diffusion coefficients and permanent charge densities) must also be averaged (i.e., effective parameters). Of course, they—most importantly the permanent charge profile $P(x)$—are also spatial averages, and so they are effective parameters in that sense as well.

The essential postulate of PNP theory is that the average potential of the Nernst-Planck equations is described by the average potential of the Poisson equation and its effective parameters (listed in note 4 and Eq. 20). Similar mean field approximations are widely used in many fields of science (See citations in Eisenberg, 1996a). The closely related Vlasov equation of plasma physics is derived from statistical mechanics in Balescu (1963, 1975). Balian (1992), Kersch and Morokoff (1995), and Syganow and von Kitzing (1995) use a generalized Vlasov model essentially the same as our PNP theory to describe the open channel.

Determining parameters

The MINPACK version of the Levenburg-Marquardt algorithm (Johnson and Faunt, 1992; Press et al., 1992, p. 683; Moré et al., 1980), performed

the least-squares fitting, converging in some two to four iterations per parameter, when starting from a reasonable but not ideal initial guess. The curve fit to the four-parameter macrodipole model (see Eq. 20) took some 8 h of cpu time; the curve fit to the seven-parameter SVD model (see Eq. 14) took some $(7/4)^2 \times 8 = 24$ h on our workstation, an IBM RS/6000 model 550, with a floating point performance of some SPECfp92 = 72.

The SVD calculation was done with a corrected and tuned version of the routine in Press et al. (1992). The SVD analysis of the four-parameter macrodipole model (see Eq. 20) took some 45 min, and the seven-parameter SVD model (see Eq. 14) took some $(7/4)^2 \times 3/4 = 2.2$ h to compute on our system.

Comparing the data set of Kienker and Lear (1995) with the flux predicted by the PNP equations for one set of adjustable parameters[10] requires the computation of some 15 IV curves, one for each solution, each containing 201 individual IV points (which are samples of the more or less continuous IV curve actually measured). The data set includes, of course, all of the information sometimes plotted as curves of reversal potential versus concentration and (the operationally-defined chord or slope) conductance (i.e., $[\Delta I/\Delta V]_{I = 0}$ or $[\partial I/\partial V]_{I = 0}$) versus concentration.

It is important to state the "ground rules" of these comparisons of theory and experiment. The distribution of permanent charge; the length, radius, and dielectric constants of the channel protein; and the diffusion coefficients in the channel's pore are the same at all potentials and in all solutions. Indeed, no parameters of the model are changed from solution to solution or applied potential to potential, other than the concentrations and applied potentials themselves. Unless otherwise indicated, only four parameters were adjusted to fit the data, namely, the two diffusion coefficients in the channel's pore D_K and D_{Cl} and the two values of the permanent charge P_1 and P_2:

$$P_1 \equiv P(0 \leq x \leq x_1) = -([d - x_2]/x_1)P(x_2 \leq x \leq d);$$

$$P_2 \equiv P(x_1 < x < x_2). \tag{13}$$

The optimal values of the diffusion coefficients D_K and D_{Cl} and the parameters of $P(x)$ are determined by minimizing the summed-square deviation between experimentally observed and theoretically predicted current. Because the PNP equations are strongly nonlinear (see Fig. 11), nonlinear least-squares curve fitting was used rather as it was used some time ago by Eisenberg (1967) and Valdiosera et al., (1974) in another context. As we shall see, the number and type of parameters needed to characterize $P(x)$ were determined using a newer method, kindly brought to our attention by Prof. Nonner (Franciolini and Nonner, 1994), singular value decomposition (SVD for short). For example, if $P(x)$ is the type of macrodipole shown in Fig. 6, characterized by parameters x_1 and x_2 (the location of the steps in charge) and charge densities P_1, P_2, and P_3 (defined later in Eq. 15), SVD shows that the Kienker-Lear data set allows measurement of two parameters of the macrodipolar charge distribution—e.g., P_1 and P_2—and the two diffusion coefficients of the ions—D_K and D_{Cl}—but the existing data do not allow reliable estimation of x_1 and x_2 themselves. No attempt was made to optimize the values of the other parameters in the theory, namely r and d (see note 19).

Singular value decomposition

The SVD is useful for us because it provides a rigorous and easy way to determine the number of (linearly independent) parameters that can be estimated from an existing data set. Without SVD, this is a difficult problem (Hamilton, 1964). The SVD is essentially a linear analysis, however, so it provides this information only in one neighborhood at a time. That is to say, SVD tells how many parameters can be independently determined in the vicinity of some particular values of those parameters, say,

$$\{\beta_j(\text{SVD})\} \equiv \{D_K, D_{Cl}|x_1, x_2|P_1, P_2, P_3\}, \tag{14}$$

where

$$P_1 \equiv P(0 \leq x \leq x_1); \quad P_2 \equiv P(x_1 \leq x \leq x_2);$$

$$\tag{15}$$

$$P_3 \equiv P(x_2 \leq x \leq d),$$

as defined in Fig. 6. Note that for the singular value decomposition, we use a larger parameter set than used in the final curve fit: the final parameter set is a subset of parameters that is well determined according to the SVD. In particular, for the SVD we allow the locations x_1; x_2; x_3 to vary and we do not require the charge on the two ends of the macrodipole to be equal; i.e., in the SVD, P_1 does not equal $-([d - x_2]/x_1)P_3$. Åqvist et al. (1991) and Sitkoff et al., (1994, and references cited therein) discuss the chemical evidence for the equality of charge at the two ends of α-helices.

Not all data sets have the same effect on the SVD. IV relations measured in some solutions (e.g., asymmetrical solutions) are far more useful in defining parameters than in others (e.g., symmetrical solutions). The SVD reflects this intuitive reality: it gives different results, depending on the bathing solution in which the data set is measured. Indeed, much of the art of experimentation is to choose experimental conditions (and variables to be measured) that yield well-determined estimates of the parameters of interest. SVD serves as a theoretical foundation for experimental design; it buttresses the experimental superstructure with objective pillars, estimates of error.

Here is how we have performed the singular value decomposition of a curve fit of PNP to data. The inputs to the theory are 1) the structure of the channel (its permanent charge, diffusion coefficients, length, diameter, and dielectric constants; see Eq. 14 above); and 2) experimental conditions (i.e., bath concentrations $C_j(L)$ and $C_j(R)$ and transmembrane potential V_{appl}). The outputs of the theory are the predicted IV relations $I(V_{\text{appl}}|C_k(L);$ $C_k(R)|\beta_i)$. This forward mapping can be represented symbolically (see Eisenberg, 1996a). When we use the theory to estimate the adjustable parameters β_j, we consider the inverse mapping shown in Fig. 1.

We use SVD to construct a linear approximation to the above inverse mapping near values β_j (of diffusion coefficients and the permanent charge) that together fit the data. For example, we might determine the best least-squares estimate of the parameters $\{D_K, D_{Cl}|x_1, x_2|P_1, P_2, P_3\}$ by the (nonlinear) Levenberg-Marquardt procedure and then linearize and perform SVD around those values. Fig. 2 shows the least-squares linear approximation to the inverse operator (derived in many texts on linear least squares, e.g., Clifford, 1973). Here, the column vector $[I_n]$ lists all of the N measured currents being used to fit the data. The currents might come from different experiments with different membrane potentials and/or bath concentrations. The column vector $[\hat{\beta}_j]$ of J adjustable parameters is the best nonlinear least-squares estimate of the value of these parameters. J might be called a "Jacobian" or sensitivity matrix, with elements $\partial I_n/\partial \beta_j$ giving the derivative of the data with respect to each adjustable parameter. $\mathbf{J}^T$ is its transpose, and the superscript -1 indicates the inverse matrix operation.

INVERSE   Inputs   Least Squares   Outputs
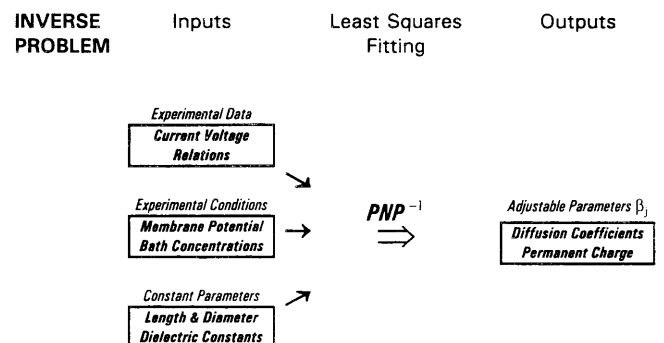**PROBLEM**   Fitting

FIGURE 1   The inverse problem by which the PNP equations are used to estimate (parameters of) the structure of the channel and the diffusion coefficients of ions.

INVERSE PROBLEM (linearized)

FIGURE 2   A linearized version of the inverse problem.

Note that some parameters may not be well determined by the combination of data and theory (as will turn out to be the case for x_1 and x_2 in the present situation).

In practical applications, experiments are usually designed to yield redundant data, thereby reducing the effect of noise and uncertainty; specifically in our case, the number of current samples far exceeds the number of adjustable parameters in the PNP equations. The matrix $[\mathbf{J}^T\mathbf{J}]$ is then nearly singular (because many of the data are redundant, rows/columns of the matrix are linearly dependent, and so different combinations of parameters can fit the somewhat noisy experimental data equally well).

The problem is how to define the inverse of the nearly singular matrix. The SVD solves the problem: it is the best estimate, in the least-squares sense, of the underdetermined parameters of theory; it provides the best approximation to the inverse of the overdetermined system of equations (see Press, et al., 1992, p. 670, for discussion and implementation; van Huffel and Vandewalle, 1991, for references and proofs; Kalman, 1996, provides a wonderful overview; Horn and Johnson, 1985, pp. 415–417, is valuable; Golub and van Loan, 1983, is the classic reference).

The SVD provides the singular values $\{s_r\} = \{s_1, s_2, \ldots, s_r, \ldots, 0, 0, \ldots, 0\}$. The number of zeros in the vector $\{s_r\}$ is the number of parameters that are not well determined by the data.[11] In this way, the singular values in $\{s_r\}$ tell how many but not which parameters are well determined; a single SVD does not directly tell which parameters are well determined by the data, because the parameters are combined (linearly) in the curve-fitting process.

The well-determined parameters are identified by considering the singular values of a model and the correlation coefficients between its parameters (shown in Table 2). The number of redundant parameters is determined from the vector $\{s_r\}$. The ill-determined parameter(s) are identified by eliminating parameters from the set $\{\beta_j\}$, one at a time. The SVD is then performed on each of the correspondingly reduced problems, with sensitivity matrices $\mathbf{J}$[one fewer parameter], $\mathbf{J}$[two fewer parameters], ... (with parameter sets $\{\beta_{j-1}\}$ $\{\beta_{j-2}\}$, ..., etc.). When all of the singular values of a reduced matrix are significantly larger than zero, the corresponding set of parameters is well determined. In other words, one chooses the largest set of parameters that give a set of singular values all significantly larger than zero.

More than one set of well-determined parameters may exist for a given data set, because any linear orthogonal transformation of well-determined parameters is also well determined. The correlations between parameters are different, however, for the different sets, and this fact helps distinguish between the sets. Of course, physical, biological, and structural information helps even more. That is in fact why in this paper we constrain the total charge to be equal on the two sides of the channel protein (see Eq. 13).[12]

Quality of fit is measured by

$$\sigma^2(I_N) \equiv \text{var(curve fit)}$$

$$\qquad\qquad\qquad\qquad (16)$$

$$\equiv \frac{1}{N} \sum_{n=1}^{n=N} [I_n(\text{theory}) - I_n(\text{experiment})]^2.$$

$\sigma^2(I_N)$ is the variance of the fit between theory and experiment (not to be confused with the variance σ_j^2 of the parameters β_j).

Chemical solutions

In all calculations the concentration variables C_j were actually activities estimated as if they were properties of bulk solution (e.g., Kienker and Lear, 1995). No one knows how to compute activity coefficients inside a channel a priori or in concentrated (i.e., physiological) ionic solutions outside a channel in an ordinary bulk solution, for that matter. Indeed, there is a considerable controversy about how to compute changes in activity when mixtures of solutes are present in different concentrations in different regions of a solution, even in well-defined physical systems of bulk phases at equilibrium (see the 18 references cited in Krukowski et al., 1995). Away from equilibrium, where large fluxes flow, just defining the appropriate variables (analogous to free energy or activity) is a significant challenge to statistical mechanics that evidently has not yet been met (Keizer, 1987; Schönert, 1994; Lee and Rasaiah, 1994; Vlad and Ross, 1995).

RESULTS

Ionic channels are often named by their selectivity (for example, as K^+ or anion channels), and their selectivity is characterized by a single number, as a rule, using "constant field" theory (Hille, 1992), however much that rule of constant field has been "proved"[13] by its exceptions. The LS channel is one of those numerous exceptions. Kienker and Lear (1995) find that the apparent selectivity P_K/P_{Cl} of the LS channel depends dramatically on ionic conditions. Figs. 3 and 4 show current-voltage relations recorded by them in symmetrical and asymmetrical solutions. (Kienker and Lear recorded IV curves as more or less continuous functions, and 201 samples were taken from each for our analysis. Only a subset of these 201 points is shown in each graph for appearance's sake.) Perhaps Fig. 5 shows the most striking result, namely the change in reversal potentials when the (approximately) 114 mM and 1040 mM solutions are interchanged from the C-terminal (in)side of the channel or the N-terminal (out)side.[14] Then the reversal potential changes from -37 mV to $+18$ mV. Fig. 5 also shows the currents carried by individual ions i_K and i_{Cl}. The intuitive idea of selectivity is a measure of the relative size of the driving force for each ion when the applied potential is the reversal potential, the potential at which the total current through the channel (carried by both ions) is zero. If $|V_{rev} - V_K| \ll |V_{rev} - V_{Cl}|$, the reversal potential for the channel approaches the equilibrium potential for K^+ and the channel is said to be a K^+ channel (where $V_{K,Cl}$ is the equilibrium (i.e., Nernst) potential for each ion). If $|V_{rev} - V_{Cl}| \ll |V_{rev} - V_K|$, the reversal potential for the channel approaches the equilibrium potential for Cl^- and the channel is said to be

a

Current voltage relations

for symmetric solutions

□ $[KCl]_N$=0.171, $[KCl]_c$=0.175 M
o $[KCl]_N$=0.0915, $[KCl]_c$=0.0943
—— PNP
- - - PNP

Single-Channel Current (pA)

Membrane Potential (mV)

b

Current voltage relations

for symmetric solutions

□ $[KCl]_N$=0.605, $[KCl]_c$=0.605 M
o $[KCl]_N$=0.323, $[KCl]_c$=0.321
—— PNP
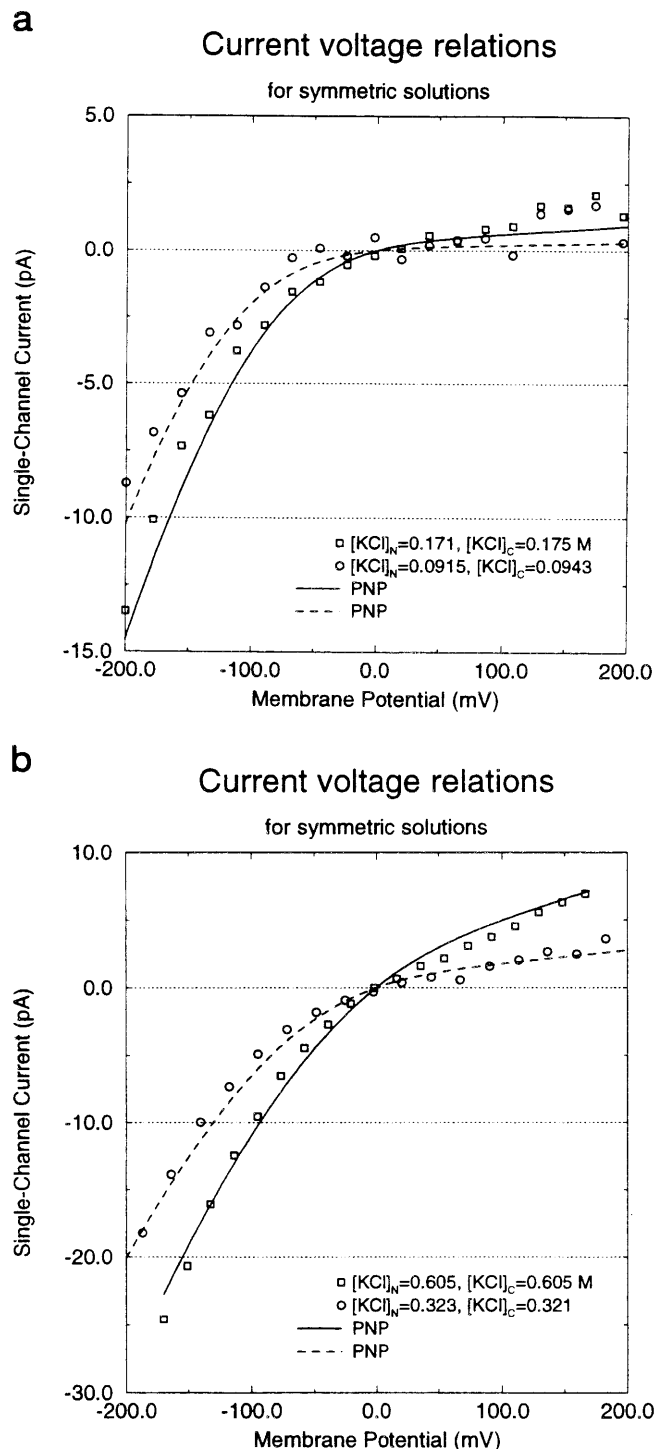- - - PNP

Single-Channel Current (pA)

Membrane Potential (mV)

FIGURE 3   Current-voltage relations in symmetrical solutions. The current flowing through a single open LS channel is shown as a function of V_{appl}, i.e., the transmembrane potential for several different solutions. $[KCl]_N$ means the concentration of [KCl] on the N-terminal or inside of the channel; $[KCl]_C$ means the concentration on the C-terminal or outside. IV curves were measured by Kienker and Lear (1995) as more or less continuous functions, and 201 samples were taken from each for our analysis. Only a subset of these 201 points is shown in each graph for appearance's sake. The theoretical curves, labeled PNP, were computed from the least-squares fit of the PNP equations as described in the text and the caption to Fig. 7.

a Cl^- channel. The current flow of each ion has the same magnitude at the reversal potential (otherwise the total current could not be zero), but the driving force needed to make the current zero is not the same. Less driving force is needed if the magnitude of the "conductance at reversal" for K^+ (defined as, say, $g_{rev}(K) \equiv i_K/(V_{rev} - V_K)$) is greater than the analogous conductance for Cl^-. In other words, the channel is selective for the ion with the greater conductance at the reversal potential.

Fitting data

Fig. 6 (lower panel) shows the structure of the LS channel (Wasserman, personal communication; Lear et al., 1988) and its pore, approximated (see thick gray lines in the figure) as a circular cylinder, with length $d = 30$ Å and radius $r = 4$ Å. The atoms that appear within the channel are actually projections of atoms within the walls of the channel. The channel was designed to be a bundle of α-helices that can be described more or less as a macrodipole (Kienker et al., 1994; Kienker and Lear, 1995), with equal amounts of permanent charge at each end (Wada, 1976; Hol, 1985). In the PNP equations used here, the three-dimensional distribution of permanent charge of a protein is represented by the one-dimensional (effective) parameter $P(x)$[15]: in particular, we describe the chemical structure of the LS channel as three steps in $P(x)$ (Fig. 6).

The charge density (per unit length) at the N or in or left side of the channel protein is $P_1 \equiv P(0 \leq x \leq x_1)$. The total charge at one end of a macrodipole is supposed to equal the charge at the other (that is, after all, what we mean by "dipole" or "macrodipole," strictly speaking; however, see note 12), and the diameter of the channels is supposed to the same everywhere. Thus,

macrodipole charge density is

$$P_1 \equiv P(0 \leq x \leq x_1) = -\frac{(d - x_2)P(x_2 \leq x \leq d)}{x_1}. \tag{17}$$

The charge density in the central region of the channel $P_2 \equiv P(x_1 < x < x_2)$, bracketed by the macrodipole, probably comes from the hydroxyl groups of the serine residues of LS.[16] But it might also come from other local properties of the LS channel protein (Åqvist et al., 1991; Sitkoff et al., 1994, and references cited therein).

The fixed charge of the LS protein is, of course, shielded by surrounding ions, as discussed semiquantitatively by Kienker and Lear (1995); in general, we use the PNP equations to quantitatively understand and predict the shielding of the fixed charge by (mobile) ions in the bathing solution and in the channel's pore.[17] Poisson-Boltzmann theory also describes such shielding, but PNP is valid away from equilibrium, in the presence of flux, where channels usually work, and Poisson-Boltzmann is not.
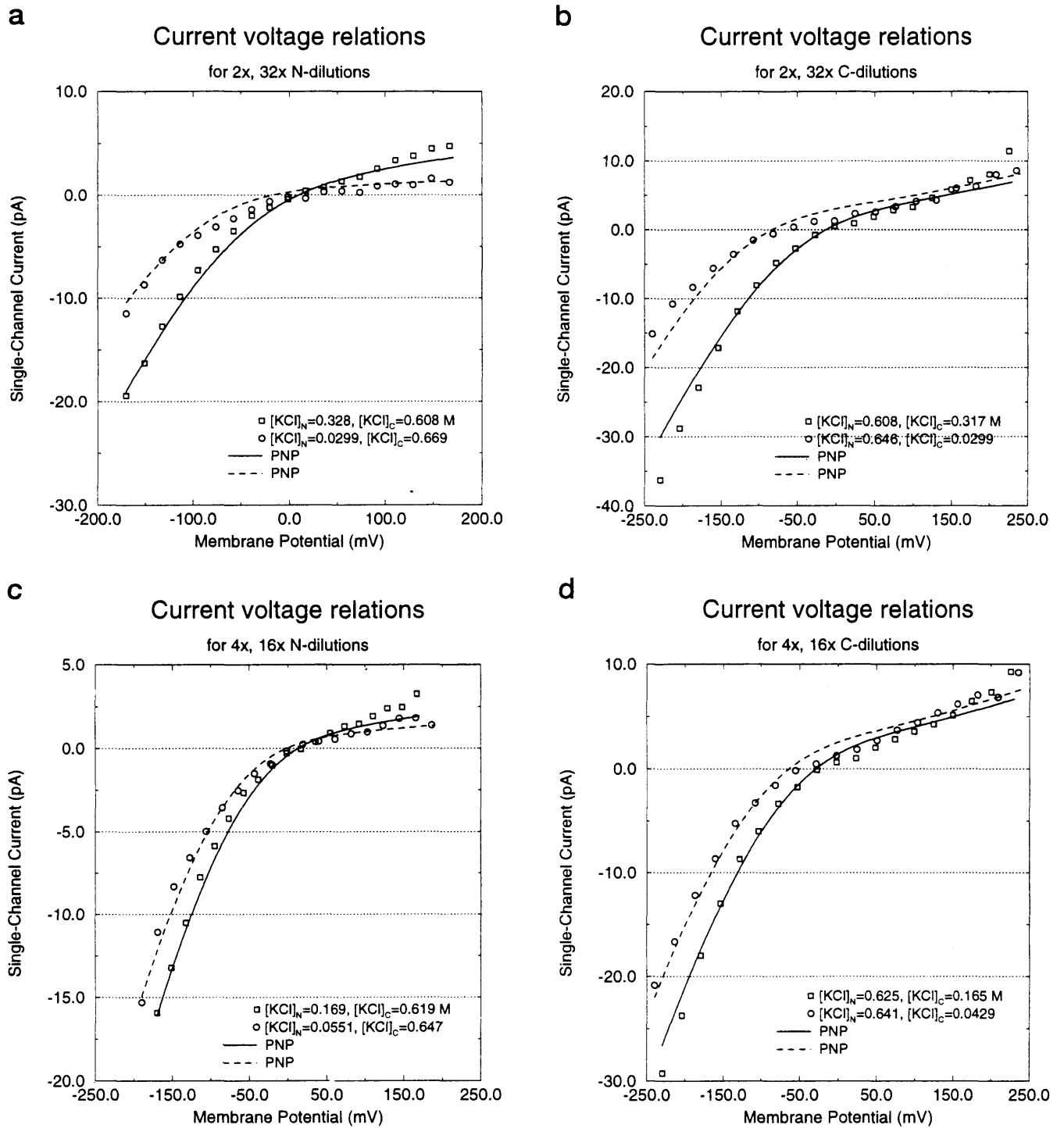
a

Current voltage relations

for 2x, 32x N-dilutions

Single-Channel Current (pA)

Membrane Potential (mV)

□ [KCl]$_N$=0.328, [KCl]$_C$=0.608 M
o [KCl]$_N$=0.0299, [KCl]$_C$=0.669
——— PNP
- - - · PNP

b

Current voltage relations

for 2x, 32x C-dilutions

Single-Channel Current (pA)

Membrane Potential (mV)

□ [KCl]$_N$=0.608, [KCl]$_C$=0.317 M
o [KCl]$_N$=0.646, [KCl]$_C$=0.0299
——— PNP
- - - · PNP

c

Current voltage relations

for 4x, 16x N-dilutions

Single-Channel Current (pA)

Membrane Potential (mV)

□ [KCl]$_N$=0.169, [KCl]$_C$=0.619 M
o [KCl]$_N$=0.0551, [KCl]$_C$=0.647
——— PNP
- - - · PNP

d

Current voltage relations

for 4x, 16x C-dilutions

Single-Channel Current (pA)

Membrane Potential (mV)

□ [KCl]$_N$=0.625, [KCl]$_C$=0.165 M
o [KCl]$_N$=0.641, [KCl]$_C$=0.0429
——— PNP
- - - · PNP

FIGURE 4   Current-voltage relations in asymmetrical solutions. The current flowing through a single open LS channel is shown as a function of V_{appl}, i.e., the transmembrane potential for several different solutions. [KCl]$_N$ means the concentration of [KCl] on the N-terminal or inside of the channel, [KCl]$_C$ means the concentration on the C-terminal or outside. The theoretical curves, labeled PNP, were computed from the least-squares fit of the PNP equations as described in the text and the caption to Fig. 7. *IV* curves were measured by Kienker and Lear (1995) as more or less continuous functions, and 201 samples were taken from each for our analysis. Only a subset of these 201 points is shown in each graph for appearance's sake.
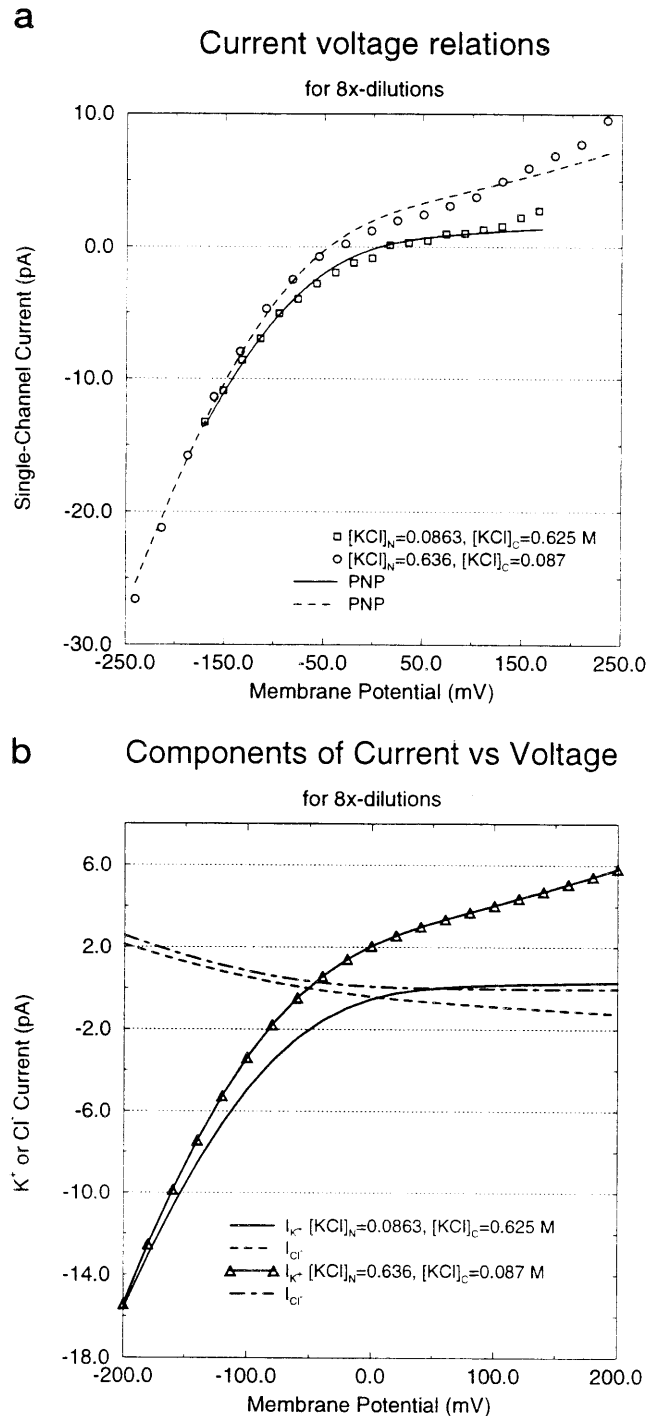
a

Current voltage relations

for 8x-dilutions

b   Components of Current vs Voltage

for 8x-dilutions

FIGURE 5   Current-voltage relations in asymmetrical solutions. (a) The current flowing through a single open LS channel is shown as a function of V_{appl}, i.e., the transmembrane potential for several different solutions. $[KCl]_N$ means the concentration of [KCl] on the N-terminal or inside of the channel; $[KCl]_C$ means the concentration on the C-terminal or outside. The theoretical curves, labeled PNP, were computed from the least-squares fit of the PNP equations as described in the text and the caption to Fig. 7. IV curves were measured by Kienker and Lear (1995) as more or less continuous functions, and 201 samples were taken from each for our analysis. Only a subset of these 201 points is shown in each graph for appearance's sake. (b) The currents carried by individual ions i_K and i_{Cl} are shown. The ratio of the magnitude of these currents is one unambiguous measure of selectivity, although it depends on "driving force" (i.e., gradient of electrochemical potential) as well as on channel properties.

SVD analysis

An SVD analysis was performed as described in the Theory and Methods section. The parameters used in the SVD analysis were the diffusion coefficients, locations, and densities of permanent charge, respectively. In this SVD analysis, P_1, P_2, and P_3 are adjustable parameters. They are not constrained by Eq. 17.

Preliminary parameters of the SVD are $\{\beta_j(\text{SVD})\}$ = $\{D_K, D_{Cl}|x_1, x_2|P_1, P_2, P_3\}$, with best fit values

$$\{\beta_j(\text{SVD})\} \cong \{D_K = 9.7 \times 10^{-7},$$

$$D_{Cl} = 8.4 \times 10^{-7}\text{cm}^2\text{s}^{-1}|x_1 = 5.7,$$

$$x_2 = 27.9 \text{ Å}|P_1 = 0.36, \quad \bullet \tag{18}$$

$$P_2 = -0.19, P_3 = -5.5 \text{ M}\}.$$

The standard deviation of the fit σ_j (preliminary) = 0.256 pA (see Eq. 16). Note that these preliminary values are not final, because two of the singular values were much smaller than the largest (Press et al., 1992, p. 672):

Preliminary singular values

$$\{1.2 \times 10^7; 8.6 \times 10^5; 2.7 \times 10^4; 3.4 \times 10^3;$$

$$2.7 \times 10^2; 28; 0.94\}. \tag{19}$$

The existence of singular values that are a small fraction[18] of the largest shows that the matrix is nearly singular, i.e., the system is overdetermined. In this situation, the parameter values and resulting fits are not terribly meaningful, and so it is necessary to trim the number of parameters, lest our numerical results be contaminated by the singular nature of (some of the) matrix operations arising (in part) from the poorly determined parameters.

On physical grounds we require the channel to be more or less a macrodipole, with equal but opposite charges at the two ends (see Eq. 17 and note 12). We see how well this simple model of the protein can fit the IV relations measured in 15 solutions. We also choose to delete the locations x_1 and x_2 from the set of adjustable parameters. The reduced (four-parameter) model is then evaluated by SVD to confirm that it is not singular. Finally, we verify that the reduced macrodipole model can fit the data with reasonable parameter values. The macrodipole model has four adjustable parameters $\beta_j(\text{MD})$:

Macrodipole parameter set

$$\{\beta_j(\text{MD})\} = \{D_K, D_{Cl}|P_1, P_2\}$$

$$\cong \{2.1 \times 10^{-6}, 2.6 \times 10^{-7} \text{ cm}^2\text{s}^{-1}|0.71, 0.47 \text{ M}\}. \tag{20}$$

The four singular values of this set are

Macrodipole singular values

$$\{6.1 \times 10^6; 3.8 \times 10^5; 1.7 \times 10^4; 3.9 \times 10^2\}. \tag{21}$$

Permanent Charge Profile
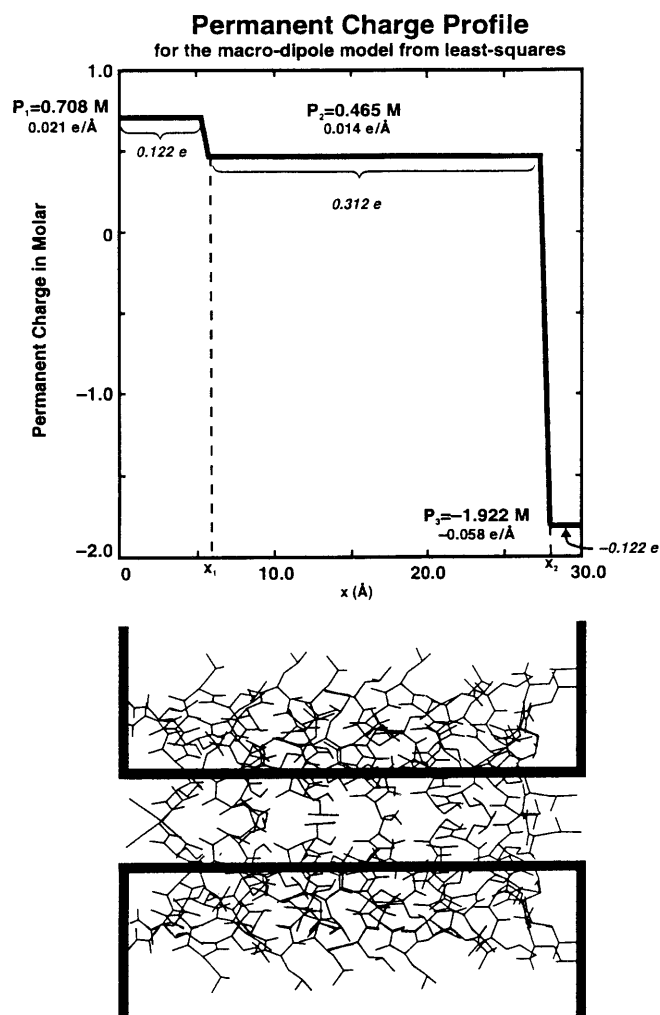### for the macro-dipole model from least-squares

FIGURE 6 Permanent charge density and structure of the LS channel. *(Bottom)* Chemical structure of the channel (Wasserman, personal communication; Lear et al., 1988), with each thin dark line representing a chemical bond. The dark wide line represents the structure used by the theory. *(Top)* Profile of permanent charge $P(x)$ which fits all the data. $P(x)$ is a one-dimensional representation of the permanent (i.e., fixed) charge of the protein. In the curve-fitting procedure, no parameters were changed from solution to solution or potential to potential, except the solutions and potentials themselves. The parameters were computed from the least-squares fit of the PNP equations to all the currents measured in 15 solutions shown in Table 1, allowing four parameters $\beta_j(MD)$ to vary, the two diffusion coefficients and the two parameters needed to specify permanent charge, namely $\{D_K, D_{Cl}|P_1, P_2\}$ as defined in Eq. 11. Table 2 shows the results. The absolute rms error in the curve fit is 0.25 pA, corresponding to a relative error of 3.6% rms (see text). Almost all theoretical points are within 7% of the corresponding measurement. Our best estimates of the parameters $\{D_K, D_{Cl}|P_1, P_2\}$ are $D_K = 2.1 \times 10^{-6}$ and $D_{Cl} = 2.6 \times 10^{-7}$ cm²/s, approximately 1/10 or 1/100 of their free solution values. The total charge at the ends of the macrodipole is $\pm0.12e$, giving unequal concentrations of 0.71 M $= 0.021e/\text{Å}$ on the N-side ($0 \leq x \leq 5.7$ Å) and -1.9 M $= -0.058e/\text{Å}$ on the C-side (27.9 Å $\leq x \leq 30$ Å). Thus the built-in potentials $\Phi_{bi}(0)$, $\Phi_{bi}(d)$ are not equal in our macrodipole model. In the central region (5.7 Å $< x <$ 27.9 Å), 22 Å long and 8 Å in diameter, the total charge is $0.31e$ and its concentration is $P_2 = 0.47$ $M = 0.014e/\text{Å}$.

The locations x_1 and x_2 were simply set to reasonable values, close to the SVD best fit (but ill-determined) values of Eq. 18, namely $x_1 = 5.7$ Å; $x_2 = 27.9$ Å. The standard deviation of the curve fit was σ_j (macrodipole) $= 0.256$ pA (four parameters; current-voltage relations measured in 15 solutions: 3015 data points altogether) compared with the standard deviation of the curve fit made with seven parameters $\sigma_j(SVD) = 0.256$ pA.

The best estimates of the parameters[19] of the reduced macrodipole model are

- At the ends of the macrodipole the total charge is $\pm0.12e$, giving unequal concentrations of 0.71 M $= 0.021e/\text{Å}$ on the N-side ($0 \leq x \leq 5.7$ Å) and -1.9 M $= -0.058e/\text{Å}$ on the C-side (27.9 Å $\leq x \leq 30$ Å). Thus the built-in potentials $\Phi_{bi}(0)$, $\Phi_{bi}(d)$ are not equal in our macrodipole model in most solutions.
- In the central region, the total charge is $0.31e$ and its concentration is $P_2 = 0.47$ M $= 0.014e/\text{Å}$ in that region (5.7 Å $< x <$ 27.9 Å), which is 22 Å long and 8 Å in diameter.
- The diffusion coefficients are $D_K = 2.1 \times 10^{-6}$ and $D_{Cl} = 2.6 \times 10^{-7}$ cm²/s, approximately 1/10 or 1/100 of their free solution values.

Table 2 shows standard deviation and correlation coefficients of the parameters. Note the strong correlation $\rho(D_K, P_2) \cong 0.98$ between the estimates of the diffusion coefficient D_K and the central permanent charge P_2.

Results of curve fits

Figs. 3–5 also show representative fits of the theory to most of the data taken in the solutions defined in Table 1. It is worthwhile to reiterate the rules of the curve fit. The numerical values of the diffusion coefficients and permanent charge densities are least-squares estimates; that is to say, they were found by minimizing the summed-square deviation between theoretical prediction and experimental result. All data points were treated equally, and no parameters of the theory were adjusted from solution to solution or potential to potential, except the bath concentrations and potentials themselves. Returning to those figures, we see that the fit is quite satisfactory. The standard deviation of the curve fit (per point) was σ(macrodipole) $= 0.26$ pA. The rms value of all of the measured currents was 7.0 pA, showing that the normalized error was $0.26/7 = 3.7\%$: some 95% of the theoretically predicted currents are within 2 SD (i.e., within $2 \times 3.7 = 7.4\%$) of the experimental values. The fits are also quite robust. If some of the data are removed from the data set, fits are not changed significantly.[20]

The quality of the fit of theory to data surprised us, considering the paucity of adjustable parameters and the difficulties faced by traditional theories (Kienker and Lear, 1995). The PNP equations evidently capture some properties of the channel reasonably well: the change in shielding predicted by the theory is enough to explain the measured

TABLE 1 Solution data

Symmetrical solutions			Asymmetrical solutions		
N-side ≅ C-side KCl (mM/liter) Concentration	KCl (mM/liter) Activity N-side|C-side	KCl Dilution N-side|C-side	KCl (mM/liter) Concentration N-side|C-side	KCl (mM/liter) Activity N-side|C-side
1000	605 | 605	2 × N	500 | 1000	328 | 608
500	321 | 323	2 × C	1000 | 500	608 | 317
250	171 | 175	4 × N	250 | 1000	169 | 619
		4 × C	1000 | 235	625 | 165
125	91.5 | 94.3	8 × N	114 | 1040	86.3 | 625
		8 × C	1060 | 115	636 | 87.0
70	54.5 | 56.3	16 × N	69.3 | 1080	55.1 | 647
		16 × C	1070 | 52.7	641 | 42.9
		32 × N	35.7 | 1120	29.9 | 669
		32 × C	1080 | 23.6	646 | 20.4

The activities are calculated in Kienker and Lear (1995). The solutions are named by the side of the channel which is diluted, following Kienker and Lear (1995). Thus, 8 × N means the solution on the N side is diluted 8× compared to the solution on the other side.

IV relations without invoking ad hoc mechanisms or structural or conformation changes described by many adjustable parameters.

The PNP equations are able to fit these data because the (average concentration of) ions in the channel's pore change automatically as conditions (i.e., bath concentrations and trans-membrane potential) change (see Figs. 9–11). The permanent charge on the channel protein does not change; thus the potential profile must change so it and the concentration profiles can simultaneously satisfy the Poisson and Nernst-Planck equations (and boundary conditions). A self-consistent treatment of shielding (which is what PNP is, in essence) seems sufficient to explain all of the data using a minimal set of adjustable parameters with quite reasonable values (see Discussion). Evidently, atomic details of the structure have little effect on *IV* relations shown here, but averages (of some type) of these atomic details presumably determine the effective parameters we use here to fit the data.

Inside the channel, the changes in the profiles of potential and concentration (as experimental conditions are changed) are substantial, as we shall soon see; the resulting changes in flux are larger, because flux is an exponential function of the potential profile.

Inside the channel

The following figures show potential and concentration profiles in two similar situations. Fig. 7 shows the occupancy of the channel (actually, its absolute value, given in units of elementary charge); that is to say, it shows the spatial integral of the concentration, in these same solutions, at different membrane potentials V_{appl}. The occupancy varies significantly with membrane potential and thus so does the total charge within the channel's pore (i.e., the sum of all occupancies, weighted by charge).

Fig. 8 shows the concentration profile in and near a channel in the 8 × N solutions[21] and in its mirror image, the

Occupancy vs Membrane Potential

for 8xN and 8xC dilutions

Legend:
— K⁺ for 8xN
- - - Cl⁻ for 8xN
+—+ K⁺ for 8xC
◆ - ◆ Cl⁻ for 8xC
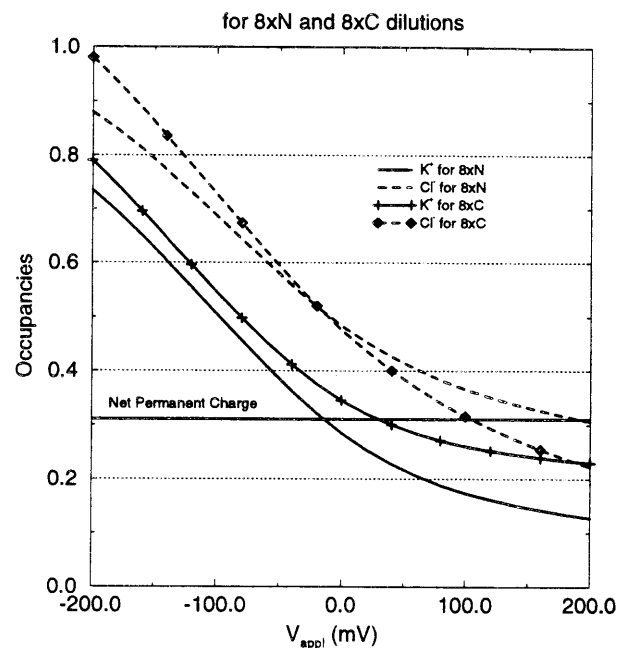
Net Permanent Charge

V_{appl} (mV)

Occupancies

FIGURE 7 The occupancy of the channel in various solutions at various membrane potentials (occupancy given in units of the elementary charge on one proton). The occupancy is defined as $\int_0^d C_K(x)dx$ or $\int_0^d C_{Cl}(x)dx$, with the concentrations computed from the PNP equations with parameters computed from the least-squares fit of the PNP equations as described in the caption to Fig. 4. The occupancy varies significantly with concentration and potential. The change in occupancy is, crudely speaking, on the order of $0.1e$ or 5% from one condition to the other. Changes in charge of this amount generally produce large changes in potential (see Figs. 10 and 11). The theoretical curves, labeled PNP, were computed from the least-squares fit of the PNP equations, as described in the text and the caption to Fig. 7.

8 × C solution defined in Table 1. In the 8 × N dilution, the channel has 114 mM KCl on the N-terminus (here left or in) side, and 1040 mM KCl on the C-terminus (here right or out) side. The equilibrium potential for K⁺/Cl⁻ is +/−132

a

Concentration along the channel

[KCl]$_N$=86.3mM, [KCl]$_C$=625mM, V=-45.7 mV

b

Concentration along the channel

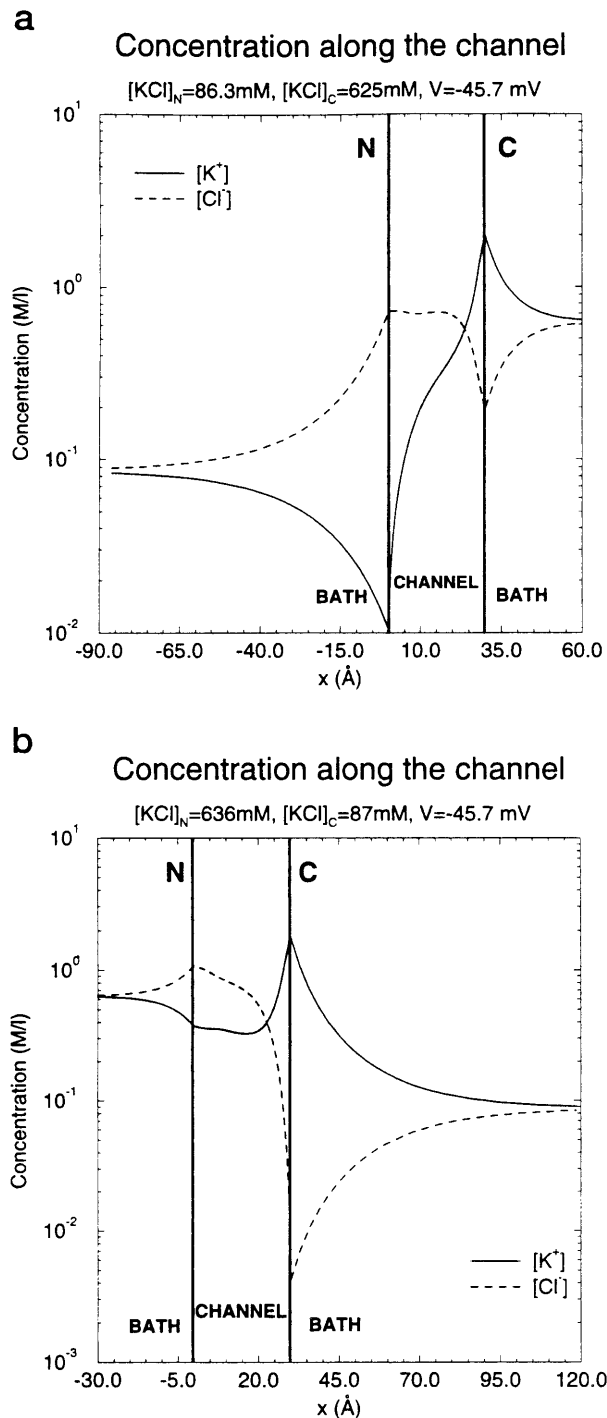[KCl]$_N$=636mM, [KCl]$_C$=87mM, V=-45.7 mV

FIGURE 8   The concentration along the channel in two different solutions. The concentration is shown in the baths, as computed by Gouy-Chapman theory, and in the channels, as computed by the PNP equations, using the parameters determined from the least-squares fit of the PNP equations, as described in the text and caption to Figure 7. The profiles of concentration vary significantly from solution to solution.

mV (inside–outside) and the reversal potential observed by Kienker and Lear was +18 mv, i.e., the channel was a K$^+$ channel. The solutions and equilibrium potentials are (approximately) interchanged to make the 8 × C dilution, but

the reversal potential found by Kienker and Lear was −37 mV. The LS channel is a better K$^+$ channel in the 8 × C solution: its reversal potential is larger in magnitude, closer to the equilibrium potential for K$^+$, in that solution. The figure shows the concentration profile computed within the channel by the PNP equations, and the concentration profile outside the channel in the baths computed by the Gouy-Chapman theory of the built-in or Donnan potential (McLaughlin, 1989; Green and Andersen, 1991).[22] Note the substantial difference in the profile in the two solutions.

Fig. 9 a shows the potential profile of a channel.[22] Fig. 9 b shows the change in the potential profile between the 8 × N and 8 × C solutions. The baths are omitted for the sake of clarity. The change in potential energy (eV) is substantial, particularly compared to the thermal energy, $k_BT \cong$ 25 meV.

Together, Figs. 8 and 9 explain why the reversal potential for the channel is different in the interchanged solutions. We need consider only K$^+$ because its (estimated) diffusion coefficient is so much larger than that for chloride that it carries most of the current. Fig. 9 a shows that the difference in potential from one side of the channel to the other is about the same in the two solutions, but Fig. 8 shows that the K$^+$ concentrations are very different in the two cases; the K$^+$ concentration is larger in the 8 × C solution and the gradient is much less. The Cl$^-$ concentrations are more or less the same in the two solutions, and so the channel is more nearly a K$^+$ channel in 8 × C solution.

Fig. 10 shows the importance of shielding.[23] The panels are computed for two different transmembrane potentials $V_{appl} = \pm100$ mV. Each panel shows three potential profiles $\varphi(x)$ predicted by the PNP equations for different contents of the channel. The short dashed lines show the potential profiles $\varphi(x)$ predicted for the 62.5 mM symmetrical solution listed in Table 1 using the parameters β_j(MD) of the macrodipole model with the values shown in Eq. 20. The solid lines show the potential profiles $\varphi(x)$ predicted when ions are absent from the surrounding baths and are excluded from the channel's pore. In this case, the permanent charge of the channel protein is not shielded by ions, but only by induced charge. The long dashed lines show the potential profile $\varphi(x)$ predicted when ions are excluded from the channel's pore but are present in the bath. In this case the Donnan or built-in potentials are present; the permanent charge of the channel is shielded by the ionic atmosphere in the baths (and by induced charge) but not by ions in the channel's pore. We conclude that shielding changes the potential profile by several k_BT/e in many locations and in many conditions.

In most theories, flux through a channel is a sensitive function of potential, i.e., of $\Phi(x) = e\varphi(x)/k_BT$. For example, flux depends exponentially on potential both in the rate theory usually used to describe open channels (Hille, 1992), and in traditional diffusion theory (e.g., Cooper et al., 1988a,b). PNP theory is no exception; the integration of the Nernst-Planck equations is unchanged by the presence of the Poisson equation, and flux depends exponentially on

a

Electric Potential Profiles

at V=-45.7 mV

b

Changes of electrical potential with

the change of solutions from 8xN to 8xC

a

Electric Potential Profiles

at V=-100 mV

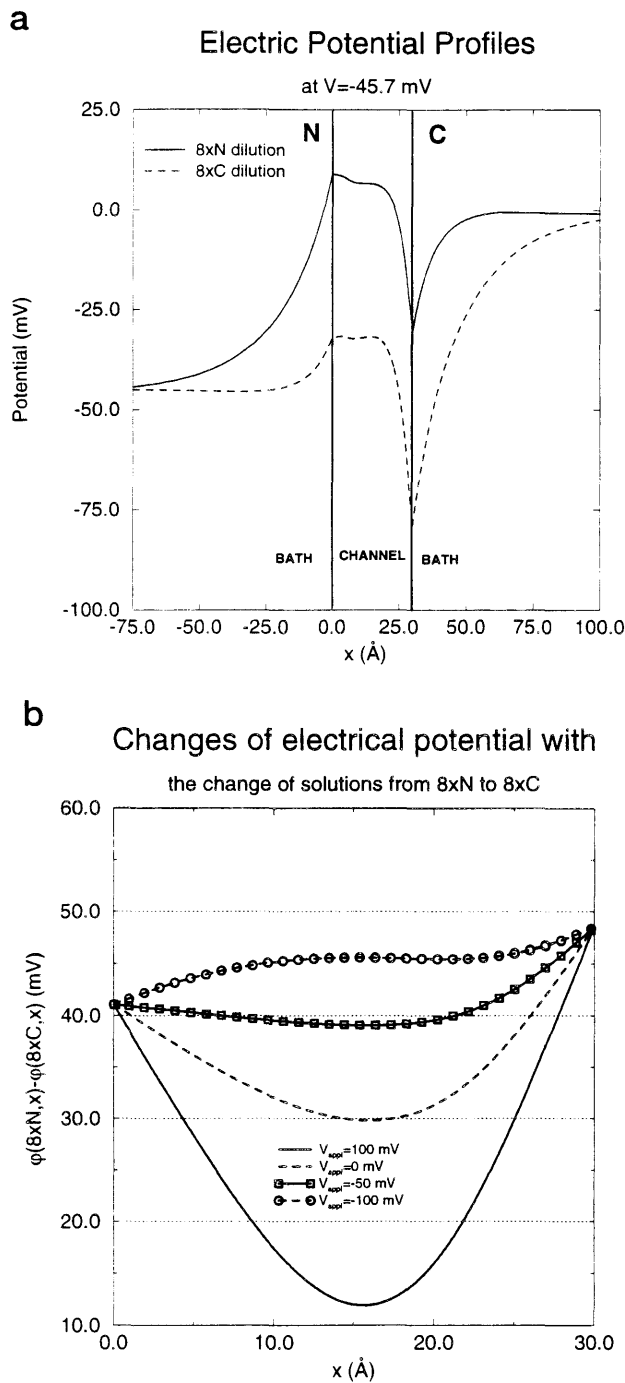
b

Electric Potential Profiles

at V=100 mV

FIGURE 9   Electrical potential as a function of position. (a) Potential in the baths computed from Gouy-Chapman theory and in the channel computed from the least-squares fit of the PNP equations as described in the text and the caption to Fig. 7. (b) Change in electrical potential as solutions are changed for different membrane potentials at different locations within the channel ($0 \leq x \leq d$). The change in potential energy (eV) is on the same order as the thermal energy, $k_BT \cong 25$ meV, at most locations. The potential profile changes significantly, even dramatically, with experimental conditions.

FIGURE 10   Three potential profiles $\varphi(x)$ predicted by the PNP equations for different contents of the channel at two different transmembrane potentials $V_{appl} = \pm 100$ mV. The short dashed line shows the potential profile $\varphi(x)$ predicted for the 62.5 mM symmetrical solution using the parameters $\beta_j(MD)$ of the macrodipole model. The solid lines show the potential profile $\varphi(x)$ predicted when ions are excluded from the channel's pore and are absent from the surrounding baths. In this case, the permanent charge of the channel protein is not shielded by ions, but only by induced charge. The long dashed lines show the potential profiles $\varphi(x)$ predicted when ions are excluded from the channel's pore but are present in the bath. In this case the permanent charge of the channel is shielded by the ionic atmosphere in the baths (and by induced charge) but not by ions in the channel's pore. We conclude that shielding changes the potential profile by several k_BT/e in many locations and in many conditions.

potential, just as it does in traditional diffusion theory; the meaning of the result is changed, however, because in PNP theory the potential within the channel is a sensitive function of experimental conditions, i.e., $\Phi(x)$ is a sensitive
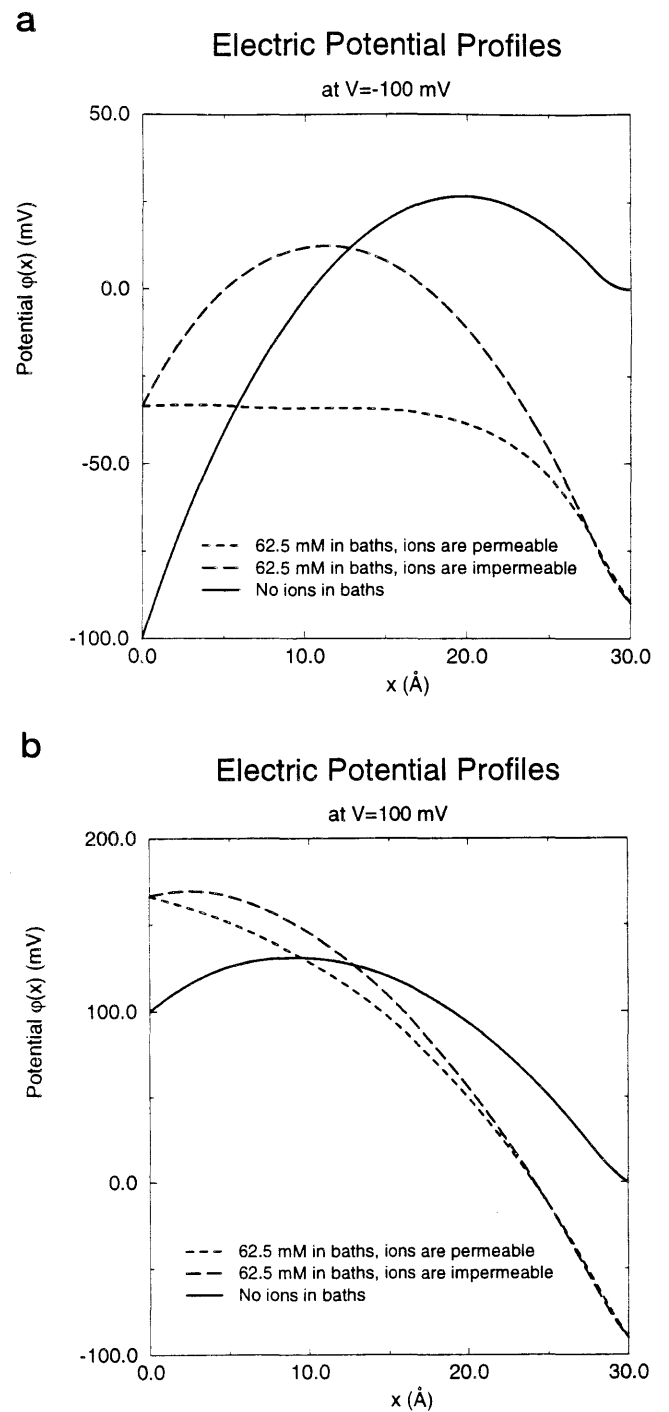
function of transmembrane potential and the bath concentrations $\Phi(x; V_{appl}; C_k(L), C_k(R))$.

The striking dependence of electric field on experimental conditions is the most important result of this paper, and is so large that it is likely to dominate all other effects in the open channel, even those that are not part of the PNP equations. Indeed, physical argument would suggest that this dependence of electrical field on bath concentration is a property to be expected of channels and proteins, whatever the theory used to describe them. If the electric field depends on bath concentration, so will the rate constants of traditional kinetic theories of enzymes (Hill, 1977, 1985; Walsh, 1979) or channels (which are nearly enzymes, Moczydlowski, 1986; Eisenberg, 1990; Andersen & Koeppe, 1992), whether we consider gating or open channel permeation.

Simplifications failed

It would be helpful if the potential profile could be separated into (a linear combination of) components, each with a definite physical meaning, particularly if one component represented the properties of the channel protein independently of the bath concentrations or applied potential. For example, in stochastic theories (e.g., Eisenberg et al., 1995; Barkai et al., 1996), the need to compute the field makes an already difficult problem nearly intractable, at least if analytical results are desired. Even in pure simulations, the dependence of the contents of the channel on the field, and the field on the contents of the channel, greatly complicates calculations (Venturi et ål., 1989).

Fig. 11 shows this separation is probably impossible; the reduced potential

$$\psi(x) \approx \varphi(x) - \overbrace{(1 - x/d)[V_{appl} + \varphi_{bi}(0) - \varphi_{bi}(d)]}^{\text{Constant field}} - \overbrace{\varphi_{bi}(d)}^{\text{Offset}}$$

$$(22)$$

remains a sensitive function of experimental conditions, even though we have subtracted the built-in potentials that depend on ionic strength in the bath and the constant field terms describing the dielectric component of V_{app}. We conclude that the nonlinear properties of the PNP equations are strongly embedded in the physics of the system and thus the theory.

DISCUSSION

Our results show that the LS channel behaves more or less as a macrodipole, with added central charge, shielded by ions in the bath and in the channel's pore, if the shielding is predicted by the PNP equations. The theory fits all of the data using just four adjustable parameters: two diffusion coefficients to describe the movement of ions in the pore of the channel; one parameter to describe the permanent charge at the ends of the channel; and another parameter to describe the permanent charge in the central region of the channel protein.

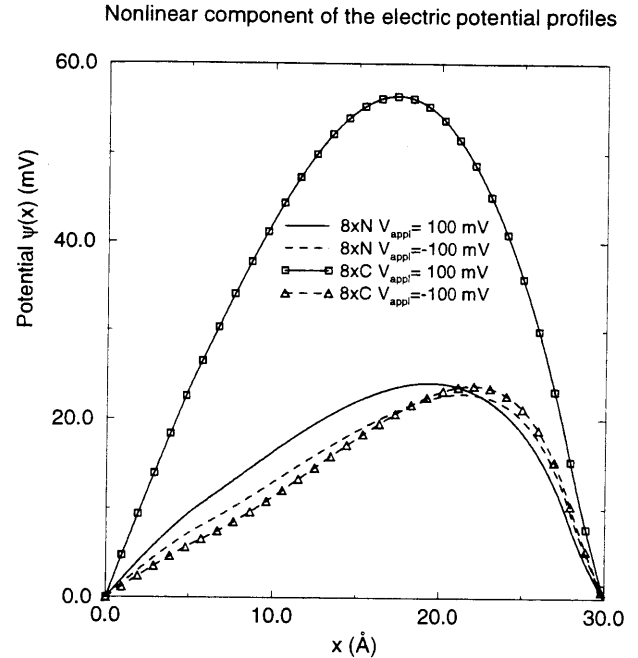Nonlinear component of the electric potential profiles

FIGURE 11 Nonlinear component $\psi(x)$ of the electrical potential under several conditions as a function of location, computed from the PNP equations with parameters determined by the least-squares fit of the PNP equations as described in the text and caption to Fig. 7, using the definition

$$\psi(x) \approx \varphi(x) - \overbrace{(1 - x/d)[V_{appl} + \varphi_{bi}(0) - \varphi_{bi}(d)]}^{\text{Constant field}} - \overbrace{\varphi_{bi}(d)}^{\text{Offset}}$$

This definition subtracts the dielectric or constant field component of the potential and the offset of the built-in or Donnan potentials, in the hope of defining a residue characteristic of the channel protein, independent of experimental conditions. The hope is not fulfilled: this residue varies substantially in shape and size with quite mild changes in experimental conditions.

It seems unlikely that any profile of charge (or any theory, for that matter) will be able to fit the *IV* data considered here, from 15 solutions, with fewer than four adjustable parameters. The permanent charge of an asymmetrical channel probably needs to be described by (at least) two parameters; the diffusion of two permeable ions needs to be described by two parameters (in the absence of an a priori theory of selectivity). The four parameters we use in the PNP equations are likely to form a minimum description of the LS channel, at least in this range of solutions, and of its selectivity, as we shall soon see.

The atomic details of the channel determine these effective parameters, of course, but (evidently) only some average of those details is important in determining open-channel *IV* relations. To the extent that those *IV* relations are the natural function of a natural channel, only those averages of atomic detail would be important in determining natural function. More than one atomic structure would give the same average parameters, and thus biological property of open channel current. Presumably, those averages would be the main phenotype of evolutionary adaptation and not the details of the atomic structure themselves.

The PNP equations fit many IV relations, with few parameters and so with little atomic detail, because the shielding of the permanent charge changes so dramatically as solutions and membrane potential are changed (Figs. 9 and 10). The contents of the channel (i.e., the permeating ions) and its potential profile change automatically when concentration and transmembrane potential change (because $C(x)$ and $\Phi(x)$ satisfy the Poisson and Nernst-Planck differential equations and boundary conditions), and this change has a significant effect on flux. The size of this effect is so large, and its physical origin is so fundamental, that a general conclusion seems inescapable: any theory of the open channel must compute the electric field—not assume it—when describing a range of experimental conditions.

Of course, PNP is not the only self-consistent theory; nor is it the best we can imagine.[24] A mean field theory (or much better, one with atomic resolution) that was computed in three dimensions, that constrained ions to a single file, or that included dehydration/resolvation would clearly be better, for example. Our work shows, however, that much atomic detail is not necessary to explain the current through single open channels: only a few parameters suffice to explain those properties in a wide range of solutions and potentials. Regrettably, no one yet knows how to compute those parameters from the atomically detailed structure of the channel and its pore.

Selectivity redefined

The ability to distinguish between different ions is one of the fundamental properties of channels (Hille, 1992). The selectivity of channels is not, however, a thermodynamic (i.e., zero flux) property of channels, but rather depends on the kinetic mechanism of permeation: substantial fluxes of different types of ions flow in channels (even at the reversal potential when total current is zero), unless the channel is perfectly selective. A quantitative treatment of selectivity requires a nonequilibrium theory of permeation (i.e., a theory predicting J_j as a function of V_{appl} in any pair of solutions $C_j(R)$ and $C_j(L)$; see Fig. 5 B), as has been said many times in the literature (e.g., Eisenman and Horn, 1983, and references cited there). To be meaningful (as opposed to phenomenological), the theory must fit the experimental data and be self-consistent. If the theory does not fit experimental data from a channel, its parameters are not a meaningful description of the channel. If the theory is inconsistent, the significance of its parameters is unclear, at best.

Traditional constant field theory is inconsistent because its derivation and solution require P_{Cl} and P_K to be constants, independent of concentration and potential, whereas experiments require P_{Cl} and P_K to be variables that depend significantly on concentration and potential. Constant field theory is also inconsistent with our results, which show that the electric field is not constant at all (Figs. 9 and 10), and that it cannot be expected to be constant in any self-consistent theory (arguments made in Eisenberg, 1996a,b). Any

spatial variation of the permanent charge will make the field change with location; any change in experimental conditions (such as bathing concentrations, the transmembrane potential, the geometrical conformation of the channel protein) is likely to change the field as well.

The PNP equations allow a more satisfying treatment of selectivity, when, as here, they fit a large and diverse data set with few parameters (four in our case). The value of those four parameters are then the best (and minimum characterization of both the channel and selectivity. More atomic detail is not necessary to characterize the IV measurements fit here. The ratio of diffusion coefficients is the best estimate of the (frictional) selectivity. In this way (diffusional or frictional) selectivity can be defined by a single number independent of bath concentration and membrane potential analogous to the permeability ratio of constant field theory. But this number measures only frictional selectivity. The selectivity produced by differences in charge on the permeant ion or its spatial distribution (in asymmetrical ions) should not be forgotten, because such electrical effects can be much larger[25] than the effects of differences in friction.

Unfortunately, estimating the selectivity—i.e., the ratio of diffusion coefficients—is not easy with the PNP equations. It requires measurements of IV relations in many solutions and curve fitting and SVD analysis, as we have seen. In our experience the estimates of diffusion coefficients are not particularly well determined by the data. The estimates change substantially when different structures of the permanent charge are input into the curve fitting process (compare Eq. 18 and 20; also note the estimates of correlation coefficients in Table 2). If one wants an easier estimate of selectivity—that can be determined from a single IV curve without curve fitting or much analysis—the traditional operational definition can be used, and indeed has surprisingly general validity (see Syganow and von Kitzing, 1995, eq. 38 and following discussion), provided one understands that the resulting parameter must be a variable—indeed, a function—depending on bath concentrations and membrane potential, as well as the properties of the channel. In particular, selectivity defined this way says nothing unique about the ratio of diffusion coefficients (i.e., "permeabilities") of individual ions in the channel. Nor does it say anything unique or simple about the underlying properties of the channel protein, e.g., the permanent charges P_1, P_2, or the size of potential barriers for different ions.

TABLE 2 Parameter estimates for the macrodipole model means, variance, and correlations

Correlation coefficient				Parameter estimate
D_K	D_{Cl}	P_1	P_2	($\pm$ SD)
1	-0.86	-0.85	0.98	$D_K = 2.11 \times 10^{-6}$ cm^2/s (± 0.02)
-0.86	1	0.55	-0.79	$D_{Cl} = 2.62 \times 10^{-7}$ cm^2/s (± 0.05)
-0.85	0.55	1	-0.84	$P_1 = 0.71$ M (± 0.004)
0.98	-0.79	-0.84	1	$P_2 = 0.47$ M (± 0.012)

The standard deviations of the estimates were determined by Eq. 32.

Role of structure

It seems clear that the PNP equations (viewed as an inverse operator; see Fig. 1) and the *IV* measurements of Kienker and Lear (1995) do not in themselves provide enough information to determine the shape of the profile of permanent charge $P(x)$.[26] However, once that shape is known from structural measurements (Åkerfeldt et al., 1993; Lear et al., 1988; Wada, 1976; Hol, 1985), the data and theory determine the parameters reasonably well (see later Discussion).

The need for structural information should not be a surprise. Even if charge and potential are related (in a simpler physical system) by just Poisson's equation, and experimental data are perfect, the same potential profile can be produced by a range of distributions of charge in many cases (i.e., for many boundary conditions). If charge and potential are related in a more complex way (as here), or data or structural information is imperfect, the ambiguity is much greater. In these situations, more than one charge distribution can produce the same potential profile across the channel. Thus, knowledge of the potential profile does not imply knowledge of the profile of permanent charge.

We, of course, have no direct way of measuring the profile of potential within a channel. But we may know it nonetheless. The observed current is a sensitive function (indeed, exponential function) of the potential profile in PNP and most other theories. If a theory predicts the observed currents at many potentials, and in many solutions, with different concentrations, the potential profiles of that theory (which it uses to calculate the current) are likely to be quite accurate if its diffusion coefficients are known and correct.

All of this presumes no knowledge of structure. But if structure is known, everything changes. If, for example, the structure of LS were fully known, and the shape of its charge distribution were determined experimentally to be that shown in Fig. 6—by x-ray diffraction, for example—there would be no ambiguity about the form of the permanent charge, only about the magnitude of the charge itself. The ambiguity in our analysis would be greatly reduced.

One might think that sufficient structural knowledge could in fact predict the values of the charge as well as the shape of its profile. And such might be the case, if the time scale on which charge were measured (by, say, crystallography) were the same as the time scale on which charge moves through a channel. The time scale of structural measurements is, however, usually seconds, minutes, or hours; the time scale of permeation is some 100 ns. The ratio of time scales is then some 10^8, and so the two measurements may see quite different distributions of charge. In particular, ions moving through channels are likely to drag charge along with them, both in adjacent waters and in nearby carbonyls (or other charged or polar groups) of the protein, forming a moving ionic atmosphere, like a "dressed ion" in free solution (reviewed in Kjellander, 1995, also see Ennis et al., 1995), together making a quasi-particle we have called a permion (Elber et al., 1995). The charge on the permion is presumably less than the charge on the permeating ion because the permanent charge on the ion is partially shielded by its "dressing," i.e., by the ionic atmosphere it drags along. For similar reasons, the charge on the protein that interacts with the permion is different from that which interacts with the ion. It too is probably reduced in magnitude because (some of the) protein charge is part of the permion; that protein charge forms some of the dressing of the ion as it is dragged along. Thus the protein charge that is effective in interaction with the permion is expected to be different, perhaps quite different from the protein charge that is effective in interaction with x-rays.

Values of parameters

Despite these caveats, we cannot resist the temptation to compare the parameter values estimated by curve fits with those expected from a simple static picture of atomic structure.

The best fit estimates of the diffusion coefficients within the channel are reasonable, being reduced some 10 or 100 times from free solution (for K^+ and Cl^-, respectively), as are most estimates of diffusion coefficients in cation-specific channels (Dani and Levitt, 1981; Hille, 1992), although the large value of the correlation coefficient (e.g., $\rho(D_K, P_2) \cong 0.98$; see Table 2) limits one's confidence.

The estimates of charge in the central region are also reasonable, although it is clearly different from the zero value expected in a macrodipole, most strictly defined. The $0.014\ e/\text{Å}$ we estimate probably arises from the hydroxyls of the serine amino acid residues of the LS protein.[27]

The estimate of the total charge at the ends of the channel ($\pm 0.12e$) is also reasonable, although quite different from the ± 2.4 or $\pm 3.0e$ found by Kienker and Lear (1995) for a channel (± 0.4 and $\pm 0.5e$ for each of the six polypeptides) and quite different from the ± 0.5 to $\pm 0.75e$ predicted by classical macrodipole theory (Hol, 1985) for a single polypeptide.

The disagreement in values of charge at the ends is large and might have no particular significance, of course, if it arose from the errors in PNP theory or in curve fitting. Or the disagreement might simply reflect our ignorance of the structure of the LS channel (which has not yet been crystallized or studied by x-ray crystallography) and of its distribution of charge. Or the protein may not be the sole bearer of permanent charge; adjacent lipids of the bilayer (e.g., that have surprisingly mobile headgroups; See-wing Chiu, personal communication) might contribute to $P(x)$, particularly at its ends.

The largest source of disagreement, however, probably comes from the theory of the macrodipole itself; it is not obvious that a molecular dynamics simulation or Poisson-Boltzmann calculation of LS will give the charge distribution predicted by Hol (1985) or used by Kienker et al., (1994) and Kienker and Lear (1995). Detailed calculations from Warshel's group, which have been confirmed by a

good deal of experimental work and several more sophisticated calculations (see Sitkoff et al., 1994, and references cited there), allowed them to conclude that "previous model calculations have drastically overestimated the helix effect" (Åqvist et al., 1991, p. 2026).[28]

In any case, direct measurements of structure would allow more reliable estimates of parameter values.

Reliability of parameter values

The parameter values reported here are reliable in some ways and not in others, as is typical in nonlinear curve fitting (Graupe, 1972; Gelb, 1986). General conclusions about the charge distribution or diffusion coefficients are difficult, and conclusions independent of the assumed structure are probably impossible. Nonetheless, specific conclusions can be drawn by comparing parameter values or structures of permanent charge, using objective statistical criteria (Hamilton, 1964; Valdiosera et al., 1974) or more subjective examination of the resulting parameter values and (predicted) IV curves.

We have compared the curve fit and parameter values reported in Eq. 20 with a number of special cases and conclude that

1. The permanent charge might be a linear function of x. The permanent charge was assumed to be a linear function of position $P(x) = [(\tilde{P}_1 - \tilde{P}_0)/d]x + \tilde{P}_0$, where d is the length of the channel. In this case, the fit was only a little worse than that reported here, but the parameters are unreasonable in the sense that they do not naturally describe the chemical structure proposed by Åkerfeldt et al. (1993) and Lear et al. (1988).

2. The values of the dielectric constants cannot be determined by fitting the PNP equations to the Kienker-Lear data set. If the dielectric constants are made an adjustable parameter in the curve fitting process, least-squares minimization does not determine their value reliably; standard deviations of the estimates and correlations with other parameters are too large. We must therefore use the customary values of the dielectric constants $\varepsilon_p = 2$ and $\varepsilon_{H_2O} = 80$, as is often done in Poisson-Boltzmann calculations (Sharp and Honig, 1990; Gunner et al., 1996; Antosiewicz et al., 1994, 1995, 1996). Calculations with atomic resolution would help considerably our treatment of this issue.

3. Diffusion coefficients of ions are not equal, i.e., $D_K \neq D_{Cl}$. If diffusion coefficients were constrained to be equal, $D_K = D_{Cl}$, the theory could not fit the data at all well, even when the full set of parameters of Eq. 14 were allowed to vary and take on optimal values. Thus we can reliably conclude that $D_K \neq D_{Cl}$, even though the values of the diffusion coefficients are not particularly well determined by the data, as we have seen.

4. Diffusion coefficients of ions in the channel are not equal to their bulk value. If diffusion coefficients were constrained to their values in bulk solution (which happen to

be nearly equal for this anion and cation), the theory could not fit the data at all well, even when the full set of parameters of Eq. 14 were allowed to vary and take on optimal values. Thus we can reliably conclude that the diffusion coefficients of ions in the channel are not equal to their bulk value, even though the values of the diffusion coefficients are not particularly well determined by the data, as we have seen.

5. The permanent charge density on the N (in)side of the channel is not zero. A finite value is needed to fit the data. If the permanent charge were constrained to zero, $P_1 = 0$, theory could not fit the data at all well, even when the full set of parameters of Eq. 14 were allowed to vary and take on optimal values.

6. The permanent charge density at the ends of the channel protein is not equal to $\pm(6 \times 0.483)e$ or $\pm(6 \times 0.366)e$. If the permanent charge is set to these values (reported for the whole channel protein by Kienker and Lear, 1995), the theory could not fit the data at all well, even if the full set of parameters of Eq. 14 were allowed to vary and take on optimal values. Thus we can reliably conclude that a macrodipole of this sort will not fit the data.

7. The charge P_2 in the middle region of the channel is not zero if the macrodipole has equal charge at its two ends. If the charge at the ends of the channel were forced to be equal, and the charge in the middle were constrained to zero, the theory could not fit the data with sensible parameter values; indeed, the best-fit value of x_1 was negative.

8. The charge P_2 in the middle region of the channel cannot be zero, even if the macrodipole has unequal charge at its two ends. If the charge P_2 in the middle region of the channel is constrained to zero, but all other parameters of Eq. 14 were unconstrained, the theory could fit all of the IV data, but only by dragging x_1 (see Fig. 6) most of the way across the channel, thereby putting some charge in its middle!

9. The induced charge term of PNP (see equation 1 of Eisenberg, 1996a) is insignificant. If this term is set to zero, the theory fits the data well and the parameter values are unchanged from the values reported in Eq. 18. The induced charge is too small to have a noticeable effect.

Most biological channels are likely to be more polar than the LS channel, which is made of nonpolar amino acids with no formal charge. We find that the permanent charge of this nonpolar channel is much larger than its induced charge. The permanent charge of most biological channels will be larger still, judging from our preliminary work (see note 23) and models that have been proposed of other biological channels (which usually contain large numbers of formal charges).

It seems safe to conclude that the induced charge term is likely to be insignificant in biological channels; despite the significant efforts needed to analyze it (Barcilon, 1992; Barcilon et al., 1992; and Chen et al., 1992).

Improving estimates of parameters

More measurements of IV relations, in more bathing solutions, would obviously improve the estimates of parameter values (if the resulting data were not statistically redundant, i.e., if it were taken in "interesting" solutions). But more structural information is not needed to explain the IV measurements studied here: only a few (effective one-dimensional) parameters and the simplest self-consistent theory are needed to explain them, not a great deal of atomic detail. It is the interpretation of these parameters in terms of the detailed properties of the protein that requires more detailed theory and more detailed experiments. Different types of measurements (beyond measurements of simple IV relations) are probably needed to provide significant new experimental insights into atomic details of the channel's pore.

High-resolution measurements that depend sensitively on the distribution of charge and potential within the pore over a range of bathing solutions would be ideal. Such sensitivity might make these measurements hard to predict by the PNP equations, but if the theory did fit, that very sensitivity would allow accurate estimation of the parameter values. For example, measurements of open channel noise, over a range of frequencies, in the presence of "slow" (e.g., blocker) ions, of various concentrations, perhaps different on different sides of the channel, might provide a rich trove of experimental phenomena and data, and thus a good deal of extra information concerning the parameters of the channel, once an adequate stochastic theory of single filing is available.[29]

More structural information also would help pin down the meaning and values of the effective parameters of the channel. Ideally, simulations of molecular dynamics could use this structural information (in atomic detail) to predict experimental measurements of open-channel current. But no one knows how to perform simulations of adequate (i.e., 5–50 μs) duration (given the accumulation of round-off error that occurs when the fundamental time step is femtoseconds) and no one knows[30] how to perform simulations of adequate (spatial) size, that would allow flux and be self-consistent, i.e., that would compute the electric field from all of the significant charges in the system, including those that maintain the transmembrane potential, those in the baths 10 to 100 Å from the channel, those on the bath electrodes, and those that maintain the potential profile across the lipid membrane far from the channel.

Perhaps a more modest approach is both feasible and sufficient. Perhaps the three-dimensional structure of the channel can be used with a three-dimensional version of PNP to predict current. If such a calculation is not feasible, even a one-dimensional theory may be enough, if it is used along a curvilinear reaction path of permion motion, determined directly from the atomic detail structure (Elber et al., 1995), and not along a straight line across the membrane.

NOTES

1. By "self-consistent" we mean a theory in which the potential is computed from all the charges present—including the mobile ions, the induced (or dielectric) charge, and the permanent charge of the protein. In such theories the total charge and the electrical potential are related by Coulomb's law, or its mathematical equivalent, Poisson's equation. In one dimension, this means that the second spatial derivative of potential is equal (at every location under every condition) to the sum of all the charges at that location, scaled by the permittivity of free space. Of course, PNP is not the only or the best possible self-consistent theory. See Discussion and note 24.

2. Läuger (1991), Hille (1992), Andersen and Koeppe (1992), and Eisenman and Horn (1983) describe some of the many traditional rate constant models that assume the electric field. Levitt (1986), Cooper et al. (1988a,b), Chiu and Jakobsson (1989), Barcilon et al. (1993), and Eisenberg et al. (1995) describe diffusion theories that assume the electric field.

3. These Vlasov equations do not include permanent charge and so cannot in themselves serve as a useful description of channels, or semiconductors, for that matter. Syganow and von Kitzing (1995) generalize the Vlasov equations to include some distributions of permanent charge and use them to describe open channels.

4. Permanent charge is defined precisely as the charge present at a location when the electric field at that location is zero. In the PNP equations flux is determined by a few effective parameters: the distribution of permanent charge, the shape and size of the pore, its dielectric constants, and the diffusion coefficients of individual ions (within the channel's pore). One of the surprises of this paper is that only a handful of parameters are necessary to describe the IV relations measured under many conditions. Evidently, detailed (atomic) knowledge of the structure is not needed to predict the function of the open channel. Regrettably, the relation of the effective and atomic parameters is not yet known.

5. The hydroxyl oxygen of serine has a charge of some -0.4 to $-0.7e$ in the molecular dynamics programs CHARMM and MOIL (Brooks et al., 1983; Elber et al., 1993).

6. The solutions considered here are made of K^+ and Cl^-, respectively, i.e., $j = 1 \Leftrightarrow K^+$ and $j = 2 \Leftrightarrow Cl^-$ and have valences $z_1 = 1$ and $z_2 = -1$.

7. See note 24.

8. Written here in dimensional form, but with labels of vague dimension.

9. Note the dependence of $\bar{\varepsilon}$ on radius, resulting from the distinguished limit used by Barcilon (1992), Barcilon et al., (1992), and Chen et al. (1992).

10. See note 4.

11. Regrettably, neither we nor our colleagues have found a paper defining precisely what "zeros in the vector $\{s_r\}$" means, although such a paper may well exist somewhere in the mathematics literature. We hope the forthcoming second edition of Golub and van Loan will discuss this important matter.

12. Note, however, that our macrodipole model is not symmetrical in all respects. The charge densities $P(0)$ and $P(d)$ and thus the built-in potentials $\Phi_{bi}(0)$, $\Phi_{bi}(d)$ are not equal in what we call the macrodipole model.

13. "Tested."

14. The N-terminal side is the left or inside of the channel in our nomenclature, which preserves the usual sign conventions of channology: the potential difference ∇V of Ohm's law $\nabla V = RI_{out}$ uses the backward difference operator ∇, i.e., $\nabla V \equiv V(x_1) - V(x_2) = V(\text{inside}) -$

V(outside), and so the differential form of Ohm's law $dV/dx = -i_{out}r$ contains a minus sign, because it uses forward differences $dV \sim \Delta V \equiv V(x_2) - V(x_1) = -\nabla V$, by the conventional definition of the derivative. Here x_2 is larger than x_1; R and r are positive; outward current is positive and is named i_{out}; and the resting potential of most cells is a negative number fairly close to the Nernst or equilibrium potential for K^+, namely $V_K \equiv (RT/F)\log_e[C_K(R)/C_K(L)]$, where C_K means the activity of potassium. The LS channel is then both an inward and N-ward rectifier, passing more N-ward current than outward current for a given transmembrane potential difference $|V(x_1) - V(x_2)|$.

15. Chen et al., (1992 pp 1390–1391) and Chen and Eisenberg (1993a, pp. 1417–1420) show how $P(x)$ arises from the cross-sectional average of the three-dimensional equations.

16. See note 5.

17. And to predict and understand the shielding produced by charge induced in the polarizable matter of the lipid bilayer, channel protein, and contents of the bath and channel pore.

18. See note 11.

19. No attempt was made to optimize the radius $r = 4$ Å or length $d = 30$ Å of the pore. The value of dielectric constants could not be determined by curve fitting (see Discussion), and so they were assumed to be $\varepsilon_p = 2$ and $\varepsilon_{H_2O} = 80$. The induced charge has little effect on our results: if the entire induced charge term is set to zero (see equation 6 and discussion in Chen et al., 1992), the standard deviation $\sigma(I)$ of the curve fit changes by less than 1%. That curve fit was done with seven adjustable parameters β_j(SVD).

20. Historically, in fact, that is what was done in this collaboration. Kienker and Lear provided Chen and Eisenberg with only a subset of their data and challenged them to predict the other results. Of course, some data sets are more important in determining parameters than others. In particular, data from asymmetrical solutions are needed, in our experience, if parameters are to be reasonably determined.

21. The solutions are named by the side of the channel that is diluted, following Kienker and Lear (1995). Thus, $8 \times N$ means the solution on the N side is diluted $8\times$ compared to the solution on the other side.

22. PNP theory is in fact independent of the shape of the profiles of concentration or potential in the baths. It describes the potential produced by ions in the bath using the formalism of the built-in potential (see Eisenberg, 1996a, and references cited therein). We show the bath profiles here only as a visual indicator of the size and significance of the charge in the "ionic atmosphere" near the channel. The profiles were calculated using the usual Gouy-Chapman formula.

23. We are fortunate and grateful that Benoit Roux suggested and Mark Ratner insisted we do this calculation. The permanent charge of most biological channels will be larger still, at least judging from our preliminary work on the neuronal background anion channel (Chen et al., 1995b) and calcium release channel of sarcoplasmic reticulum (Chen et al., personal communication) where the permanent charge seems to be more than 5 M (!).

24. The limitations in the PNP theory are extensively discussed in reviews (Eisenberg, 1996a,b) and in original papers (e.g., Barcilon, 1992; Barcilon et al., 1992; Barcilon et al., Ratner 1993; Chen and Eisenberg, 1993a; Chen et al., 1995a; Eisenberg et al., 1995; Elber et al., 1995; Barkai et al., 1996). The treatment of the dielectric term is not a problem because it is so small (see note 19). The treatment of the entry/exit steps is more problematic because the dehydration and resolvation accompanying ion entry/exit are nearly phase changes for the permeating ion. The resulting change in energy of the ion may depend in complex ways on the shape of the permanent and mobile charge profile in the channel; indeed, it might depend on flux itself (Chen and Eisenberg, 1993b). We imagine that the simple approximation used here to describe the ends of the channel suffices to fit the IV data because shielding has a much larger effect on IV curves than the entry process (or most anything else; see Figs. 9–11), and. PNP describes shielding more or less correctly, even when it uses just a few parameters to describe the channel protein.

25. The correlation $\rho(D_K, P_2) \cong 0.98$ in Table 2, between the estimates of the diffusion coefficient and the central permanent charge, would refresh our memory, if we were ever to forget.

26. For example, the data can be fit with a profile of permanent charge linear in distance; see later Discussion.

27. See note 5.

28. They suggest that the overestimate is a factor of 10 or so for the energy of stabilization of HIS-18 in barnase.

29. Barkai et al. (1996) is a step in that direction.

30. If the system is an aqueous solution. Evidently, someone does know how in another system; simulations of submicron MOSFETS have computed the potential self-consistently (in atomic detail on the femtosecond time scale) for some years (e.g., Venturi et al., 1989).

REFERENCES

Åkerfeldt, K. S., J. D. Lear, Z. R. Wasserman, L. A. Chung, and W. F. DeGrado. 1993. Synthetic peptides as models for ion channel proteins. *Acc. Chem. Res.* 26:191–197.

Andersen, O. S., and R. E. Koeppe. 1992. Molecular determinants of channel function. *Physiol. Rev.* 72:S89–S157.

Antosiewicz, J., M. K. Gilson, I. H. Lee, and J. A. McCammon. 1995. Acetylcholinesterase: diffusional encounter rate constants for dumbbell models of ligand. *Biophys. J.* 68:62–68.

Antosiewicz, J., J. A. McCammon, and M. K. Gilson. 1994. Prediction of pH-dependent properties of proteins. *J. Mol. Biol.* 238:415–436.

Antosiewicz, J., J. A. McCammon, and M. K. Gilson. 1996. The determinants of pK_a's in proteins. *Biochemistry.* 35:7819–7833.

Åqvist, J., H. Luecke, F. A. Quiocho, and A. Warshel. 1991. Dipoles localized at helix termini of proteins stabilize charges. *Proc. Natl. Acad. Sci. USA.* 88:2026–2030.

Ashcroft, N. W., and N. D. Mermin. 1976. Solid State Physics. Harcourt Brace College Publishers, New York. 1–795.

Balescu, R. 1963. Statistical Mechanics of Charged Particles. John Wiley and Sons, New York.

Balescu, R. 1975. Equilibrium and Nonequilibrium Statistical Mechanics. John Wiley and Sons, New York.

Balian, R. 1992. From Microphysics to Macrophysics, Vol. 1. Springer-Verlag, New York.

Barcilon, V. 1992. Ion flow through narrow membrane channels: part I. *SIAM J. Appl. Math.* 52:1391–1404.

Barcilon, V., D. P. Chen, and R. S. Eisenberg. 1992. Ion flow through narrow membrane channels: part II. *SIAM J. Appl. Math.* 52:1405–1425.

Barcilon, V., D. Chen, R. S. Eisenberg, and M. Ratner. 1993. Barrier crossing with concentration boundary conditions in biological channels and chemical reactions. *J. Chem. Phys.* 98:1193–1211.

Barkai, E., R. S. Eisenberg, and Z. Schuss. 1996. A bidirectional shot noise in a singly occupied channel. *Phys. Rev.* in press.

Berne, B. J., M. Borkovec, and J. E. Straub. 1988. Classical and modern methods in reaction rate theory. *J. Phys. Chem.* 92:3711–3725.

Brooks, B. R., R. E. Bruccoleri, B. D. Olafson, D. J. States, S. Swaminathan, and M. Karplus. 1983. CHARMM: a program for macromolecular energy minimization and dynamics calculations. *J. Comput. Chem.* 4:187–217.

Chen, D. P., V. Barcilon, and R. S. Eisenberg. 1992. Constant field and constant gradients in open ionic channels. *Biophys. J.* 61:1372–1393.

Chen, D. P., and R. S. Eisenberg. 1993a. Charges, currents and potentials in ionic channels of one conformation. *Biophys. J.* 64:1405–1421.

Chen, D. P., and R. S. Eisenberg. 1993b. Flux, coupling and selectivity in ionic channels of one conformation. *Biophys. J.* 65:727–746.

Chen, D., R. Eisenberg, J. Jerome, and C. Shu. 1995a. Hydrodynamic model of temperature change in open ionic channels. *Biophys. J.* 69:2304–2322.

Chen, D., W. Nonner, and B. Eisenberg. 1995b. PNP Theory fits current-voltage (IV) relations of a neuronal anion channel in 13 solutions. *Biophys. J.* 68:A370.

Chiu, S. W., and E. Jakobsson. 1989. Stochastic theory of singly occupied ion channels. II. Effects of access resistance and potential gradients extending into the bath. *Biophys. J.* 55:147–157.

Clifford, A. A. 1973. Multivariate Error Analysis. John Wiley and Sons, New York.

Cooper, K. E., P. Y. Gates, and R. S. Eisenberg. 1988a. Surmounting barriers in ionic channels. *Q. Rev. Biophys.* 21:331–364.

Cooper, K. E., P. Y. Gates, and R. S. Eisenberg. 1988b. Diffusion theory and discrete rate constants in ion permeation. *J. Membr. Biol.* 109: 95–105.

Cooper, K., E. Jakobsson, and P. Wolynes. 1985. The theory of ion transport through membrane channels. *Prog. Biophys. Mol. Biol.* 46: 51–96.

Dani, J. A., and D. G. Levitt. 1981. Water transport and ion-water interaction in the gramicidin channel. *Biophys. J.* 35:501–508.

Davis, M. E., J. D. Madura, B. A. Luty, and J. A. McCammon. 1991. Electrostatics and diffusion of molecules in solution: simulations with the University of Houston Brownian Dynamics program. *Comput. Phys. Commun.* 62:187–197.

Davis, M. E., and J. A. McCammon. 1990. Electrostatics in biomolecular structure and dynamics. *Chem. Rev.* 90:509–521.

Eisenberg, R. S. 1967. Equivalent circuit of single crab muscle fibers as determined by impedance measurement with intracellular electrodes. *J. Gen Physiol.* 50:1785–1806.

Eisenberg, R. S. 1990. Channels as enzymes. *J. Membr. Biol.* 115:1–12.

Eisenberg, R. S. 1996a. Computing the field in proteins and channels. *J. Membr. Biol.* 150:1–25.

Eisenberg, R. S. 1996b. Atomic biology, electrostatics and ionic channels. *In* New Developments and Theoretical Studies of Proteins. Advanced Series in Physical Chemistry, Vol. 7. Ron Elber, editor. World Scientific, Philadelphia.

Eisenberg, R. S., M. M. Klosek, and Z. Schuss. 1995. Diffusion as a chemical reaction: stochastic trajectories between fixed concentrations. *J. Chem. Phys.* 102:1767–1780.

Eisenman, G., and R. Horn. 1983. Ionic selectivity revisited: the role of kinetic and equilibrium processes in ion permeation through channels. *J. Membr. Biol.* 76:197–225.

Elber, R. 1996. Reaction path studies of biological molecules. *In* New Developments and Theoretical Studies of Proteins. Ron Elber, editor. World Scientific, Philadelphia.

Elber, R., D. Chen, D. Rojewska, and R. S. Eisenberg. 1995. Sodium in gramicidin: an example of a permion. *Biophys. J.* 68:906–924.

Elber, R., A. Roitberg, C. Simmerling, R. Goldstein, G. Verkhivker, H. Li, and A. Ulitsky. 1993. MOIL: a molecular dynamics program with emphasis on conformational searches and reaction path calculations. *In* Statistical Mechanics, Protein Structure and Protein-Substrate Interactions. S. Doniach, editor. Plenum Press, New York.

Ennis, J., R. Kjellander, and D. J. Mitchell. 1995. Dressed ion theory for bulk symmetric electrolytes in the restricted primitive model. *J. Chem. Phys.* 102:975–991.

Fleming, G., and P. Hänggi. 1993. Activated Barrier Crossing. Applications in Physics, Chemistry and Biology. World Scientific, New Jersey.

Forsten, K. E., R. E. Kozack, D. A. Lauffenberger, and S. Subramaniam. 1994. Numerical solution of the nonlinear Poisson-Boltzmann Equation for a membrane-electrolyte system. *J. Phys. Chem.* 98:5580–5586.

Franciolini, F., and W. Nonner. 1994. A multi-ion permeation mechanism in neuronal background chloride channels. *J. Gen. Physiol.* 104: 725–746.

Gardiner, C. W. 1985. Handbook of Stochastic Methods: For Physics, Chemistry and the Natural Sciences. Springer-Verlag, New York.

Gelb, A. 1986. Applied Optimal Estimation. MIT Press, Cambridge, MA. 1–370.

Gilson, M. K., K. A. Sharp, and B. H. Honig. 1988. Calculating the electrostatic potential of molecules in solution: method and error assessment. *J. Comput. Chem.* 9:327–335.

Golub, G. H., and C. F. van Loan. 1983. Matrix Computations. Johns Hopkins University Press, Baltimore, MD. 1–476.

Graupe, D. 1972. Identification of Systems. Van Nostrand Reinhold Company, New York. 1–268.

Green, W. N., and O. S. Andersen. 1991. Surface charges and ion channel function. *Annu. Rev. Physiol.* 53:341–359.

Gunner, M. R., A. Nicholls, and B. Honig. 1996. Electrostatic potentials in *Rhodopseudomonas viridis* reaction centers: implications for the driving force and directionality of electron transfer. *J. Phys. Chem.* 100: 4277–4291.

Hamilton, W. C. 1964. Statistics in Physical Science. Ronald Press, NY.

Hänggi, P., P. Talkner, and M. Borokovec. 1990. Reaction-rate theory: fifty years after Kramers. *Rev. Mod. Phys.* 62:251–341.

Hecht, J. L., B. Honig, Y. K. Shin, and W. L. Hubbell. 1995. Electrostatic potentials near the surface of DNA: comparing theory and experiment. *J. Phys. Chem.* 99:7782–7786.

Hill, T. L. 1977. Free Energy Transduction in Biology. Academic Press, New York.

Hill, T. L. 1985. Cooperativity Theory in Biochemistry. Springer Verlag, New York.

Hille, B. 1992. Ionic Channels of Excitable Membranes, 2nd Ed. Sinauer Associates, Sunderland, MA. 1–607.

Hol, W. G. J. 1985. The role of the α-helix dipole in protein function and structure. *Prog. Biophys. Mol. Biol.* 45:149–195.

Holst, M., R. E. Kozcak, F. Saied, and Subramaniam. 1994. Treatment of electrostatic effects in proteins. Multigrid-based-Newton iterative method for solution of the full nonlinear Poisson-Boltzmann equation. *Protein Struct. Funct. Genet.* 18:231–245.

Honig, B., and A. Nichols. 1995. Classical electrostatics in biology and chemistry. *Science.* 268:1144–1149.

Horn, R. A., and C. A. Johnson. 1985. Matrix Analysis. Cambridge University Press, New York.

Hynes, J. T. 1985. Chemical reaction dynamics in solution. *Annu. Rev. Phys. Chem.* 36:573–597.

Hynes, J. T. 1986. The theory of reactions in solution. *In* Theory of Chemical Reactions, Vol. 4. M. Baer, editor. Boca Raton, FL. 171–234.

Jerome, J. W. 1996. Analysis of Charge Transport. A Mathematical Study of Semiconductor Devices. Springer Verlag, New York. 1–155.

Johnson, M. L., and L. M. Faunt. 1992. Parameter estimation by least-squares methods. *Methods Enzymol.* 210:1–36.

Kalman, D. 1996. A singularly valuable decomposition: the SVD of a matrix. *College Math. J.* 27:2–23.

Keizer, J. 1987. Statistical Thermodynamics of Nonequilibrium Processes. Springer Verlag, New York. 1–506.

Kersch, A., and W. J. Morokoff. 1995. Transport Simulation in Microelectronics. Birkhäuser, Boston.

Kienker, P. K., W. F. DeGrado, and J. D. Lear. 1994. A helical-dipole model describes the single-channel current rectification of an uncharged peptide ion channel. *Proc. Natl. Acad. Sci. USA.* 91:4859–4863.

Kienker, P. K., and J. D. Lear. 1995. Charge selectivity of the designed uncharged peptide ion channel Ac-(LSSLLSL)3-CONH2. *Biophys. J.* 68:1347–1358.

Kjellander, R. 1995. Modified Debye-Hückel approximation with effective charges: an application of dressed ion theory for electrolyte solutions. *J. Phys. Chem.* 99:10392–10407.

Klapper, I., R. Hagstrom, R. Fine, K. Sharp, and B. Honig. 1986. Focusing of electric fields in the active site of Cu, Zn superoxide dismutase. *Protein Struct. Funct. Genet.* 1:47–79.

Kramers, H. A. 1940. Brownian motion in a field of force and the diffusion model of chemical reactions. *Physica* 7:284–304.

Krukowski, A., H. S. Chan, and K. A. Dill. 1995. An exact lattice model of complex solutions: chemical potential depend on solute and solvent shape. *J. Chem. Phys.* 103:10675–10688.

Läuger, P. 1991. Electrogenic Ion Pumps. Sinauer Associates, Sunderland, MA.

Lear, J. D., Z. R. Wasserman, and W. F. DeGrado. 1988. Synthetic amphiphilic peptide models for protein ion channels. *Science.* 240: 1177–1181.

Lee, S. H., and J. C. Rasaiah. 1994. Molecular dynamics simulation of ionic mobility. I. Alkali metal cations in water at 25°C. *J. Chem. Phys.* 101:6964–6974.

Levitt, D. G. 1986. Interpretation of biological ion channel flux data. Reaction rate versus continuum theory. *Annu. Rev. Biophys. Biophys. Chem.* 15:29–57.

Lundstrom, M. 1992. Fundamentals of Carrier Transport. Addison Wesley, New York.

Mafé, S., J. Pellicer, and V. M. Aguilella. 1986. Ionic transport and space charge density in electrolytic solutions as described by Nernst-Planck and Poisson equations. *J. Phys. Chem.* 90:6045–6050.

Mason, E., and E. McDaniel. 1988. Transport Properties of Ions in Gases. John Wiley and Sons, New York.

McLaughlin, S. 1989. The electrostatic properties of membranes. *Annu. Rev. Biophys. Biophys. Chem.* 18:113–136.

Moczydlowski, E. 1986. Single-channel enzymology. *In* Ion Channel Reconstitution. C. Miller, editor. Plenum Press, New York.

Moré, J. J., B. S. Garbow, and K. E. Hillstrom. 1980. User Guide for Minpack-1. Argonne National Laboratory, Report ANL-80.

Onsager, L., and S. Machlup. 1953. Fluctuations and irreversible processes. *Phys. Rev.* 91:1505–1512.

Press, W. H., S. A. Teukolsky, W. T. Vetterling, and B. P. Flannery. 1992. Numerical Recipes in Fortran. Cambridge University Press, New York. 919.

Roulston, D. J. 1990. Bipolar Semiconductor Devices. McGraw-Hill Publishing Company, New York.

Schönert, H. 1994. Debye-Hückel theory for hydrated ions. 6. Thermodynamic properties of aqueous solutions of 1:1 chlorides between 273 and 523 K. *J. Phys. Chem.* 98:643–653.

Seeger, K. 1991. Semiconductor Physics, 5th Ed. Springer Verlag, New York.

Selberherr, S. 1984. Analysis and Simulation of Semiconductor Devices. Springer-Verlag, New York. 1–293.

Sharp, K., and B. Honig. 1990. Electrostatic interactions in macromolecules: theory and applications. *Annu. Rev. Biophys. Biophys. Chem.* 19:301–332.B.

Shur, M. 1990. Physics of Semiconductor Devices. Prentice-Hall, Englewood Cliffs, NJ. 1–660.

Sitkoff, D., D. J. Lockhart, K. A. Sharp, and B. Honig. 1994. Calculation of electrostatic effects at the amino terminus of an α-helix. *Biophys. J.* 67:2251–2260.

Spohn, H. 1991. Large Scale Dynamics of Interacting Particles. Springer Verlag, New York. 1–337.

Stratt, R. M. 1995. The instantaneous normal modes of liquids. *Acc. Chem. Res.* 28:201–207.

Syganow, A., and E. von Kitzing. 1995. Integral weak diffusion and diffusion approximations applied to ion transport through biological ion channels. *J. Phys. Chem.* 99:12030–12040.

Sze, S. M. 1981. Physics of Semiconductor Devices. John Wiley and Sons, New York. 7–838.

Tuckerman, M. N., and B. J. Berne. 1993. Vibrational relaxation in simple fluids: comparison of theory and simulation. *J. Chem. Phys.* 98: 7301–7318.

Valdiosera, R., C. Clausen, and R. S. Eisenberg. 1974. Impedance of frog skeletal muscle fibers in various solutions. *J. Gen. Physiol.* 63:460–491.

van Huffel, S., and J. Vandewelle. 1991. The Total Least Squares Problem. Society for Industrial and Applied Mathematics, Philadelphia.

Venturi, F., R. K. Smith, E. C. Sangiorgi, M. R. Pinto, and B. R. Riccó. 1989. A general purpose device simulator coupling Poisson and Monte Carlo transport with applications to deep submicron MOSFET's. *IEEE Trans. Computer-Aided Design.* 8:360–369.

Vlad, M. O., and J. Ross. 1995. Fluctuation-dissipation relations for chemical systems far from equilibrium. *J. Chem. Phys.* 100:7268–7278.

Wada, A. 1976. The α-helix as an electric macro-dipole. *Adv. Biophys.* 9:1–63.

Walsh, C. 1979. Enzymatic Reaction Mechanisms. W. H. Freeman Company, San Francisco.

Warwicker, J., and H. C. Watson. 1982. Calculation of the electric potential in the active site cleft due to alpha helix dipoles. *J. Mol. Biol.* 157: 671–679.